Diesel Exhaust Exposure in the Duwamish Study (DEEDS)

Technical Report

University of Washington
Department of Environmental & Occupational Health Sciences
Seattle, WA

September 13, 2013

Authors:
Jill K Schulte, MPH
Assaf P Oron, PhD, MS
Joel D Kaufman, MD, MPH
Julie R Fox, PhD, MHS
Sheryl Magzamen, PhD, MPH
Nancy Beaudet, MS, CIH
Timothy V Larson, PhD, MSChE

This research was funded by The Kresge Foundation, Healthy Environments Program.

Suggested Citation:
Schulte, J.K., Magzamen, S., Oron, A.P., Beaudet, N., Kaufman, J.D., Larson, T.V., & Fox, J.R. (2013). Diesel Exhaust Exposure in the Duwamish Study: Technical Report. Seattle, WA: University of Washington School of Public Health, Department of Environmental Health Sciences. Retrieved [date], from http://www.duwamishdiesel.org/home/technical-report

SCHOOL OF PUBLIC HEALTH
UNIVERSITY of WASHINGTON

Acknowledgements:
We'd like to thank our partners at Puget Sound Sage, who have been responsible for the community engagement component of DEEDS: Genevieve Aguilar, Samantha Keller, Zack Deustch-Gross, and Melanie Bin Jung. Several public agencies contributed valuable logistical support to the sampling campaigns, including the Puget Sound Clean Air Agency, the Washington Department of Ecology, Seattle City Light, King County International Airport, Seattle Parks and Recreation, and the South Seattle Community College. We are especially appreciative of the input and volunteer efforts of residents of South Park and Georgetown.

Additional Research Team Members:

Mark Davey
Amanda Gassett
Gus Glover
Timothy Gould
Anne Ho
Victoria Kalumbi
Michael Paulsen
Hamza Rabi
Miyoko Sasakura
Christopher Simpson

For more information about this report, please contact Julie Fox or Sheryl Magzamen at:

Julie Fox
University of Washington
Dept of Environmental Health & Occupational Health Sciences
richmanj@uw.edu

Sheryl Magzamen
Colorado State University
Dept of Environmental and Radiological Health Sciences
sheryl.magzamen@colostate.edu

Table of Contents

INDEX OF FIGURES

INDEX OF TABLES

INDEX OF EQUATIONS

EXECUTIVE SUMMARY

The Diesel Exhaust Exposure in the Duwamish Study (DEEDS) is a community-academic partnership between the Department of Environmental and Occupational Health Sciences (DEOHS) in the School of Public Health at the University of Washington and Puget Sound Sage. This study sought to characterize the gradient of diesel exhaust in the south Seattle neighborhoods of South Park and Georgetown. With guidance from community members and the program partner, DEOHS researchers measured levels of diesel exhaust markers in a high-density air sampling campaign, built statistical models to identify spatial features predictive of diesel exhaust, and created maps of the gradient of diesel pollution across the neighborhoods.

Two 2-week sampling campaigns were conducted in the study neighborhoods during summer 2012 and winter 2012-2013. The time periods for these campaigns were selected to capture seasonal variation in diesel pollution, other air pollution sources, and weather. Data were collected on four pollutants as markers of traffic-related air pollution: 1-nitropyrene (1-NP), a polycyclic aromatic hydrocarbon that is a by-product of combustion from diesel engines; black carbon (BC); oxides of nitrogen (NO_x); and particulate matter less than 2.5 μm in diameter ($PM_{2.5}$). Measurements of these pollutants were collected at 20 active sampling sites in South Park and Georgetown as well as 4 comparison sites in other neighborhoods. In addition, the campaign included passive sampling for NO_x and NO_2 at 99 sites and measurements of on-road carbon emissions from a mobile monitoring instrument. Active and passive samplers were co-located at the Puget Sound Clean Air Agency and Washington State Department of Ecology's Air Quality Monitoring Stations. Secondary data included traffic forecasts and meteorological information.

To determine the predictive spatial features, statistical models were derived using a hybrid land-use regression/dispersion modeling approach. Diesel gradient maps were generated by calculating pollution predictions at gridded points 50m apart, which were smoothed using universal kriging.

Results generally indicated a wide degree of variation in pollution levels across the study area. Average BC, 1-NP, NO_2 and NO_x levels were higher in December than August, though August measurements showed a greater degree of variability. Prediction models were successfully built for all pollutants except $PM_{2.5}$ and December 1-NP. These models were able to explain a very large amount of the community variation in pollutant exposure by factoring in distance to developed areas, railroads, truck traffic, and information from mobile monitoring efforts, especially for August 1-nitropyrene (cross-validated R^2 of 0.73). The modeled gradient of August 1-NP predictions is shown in Figure 1.

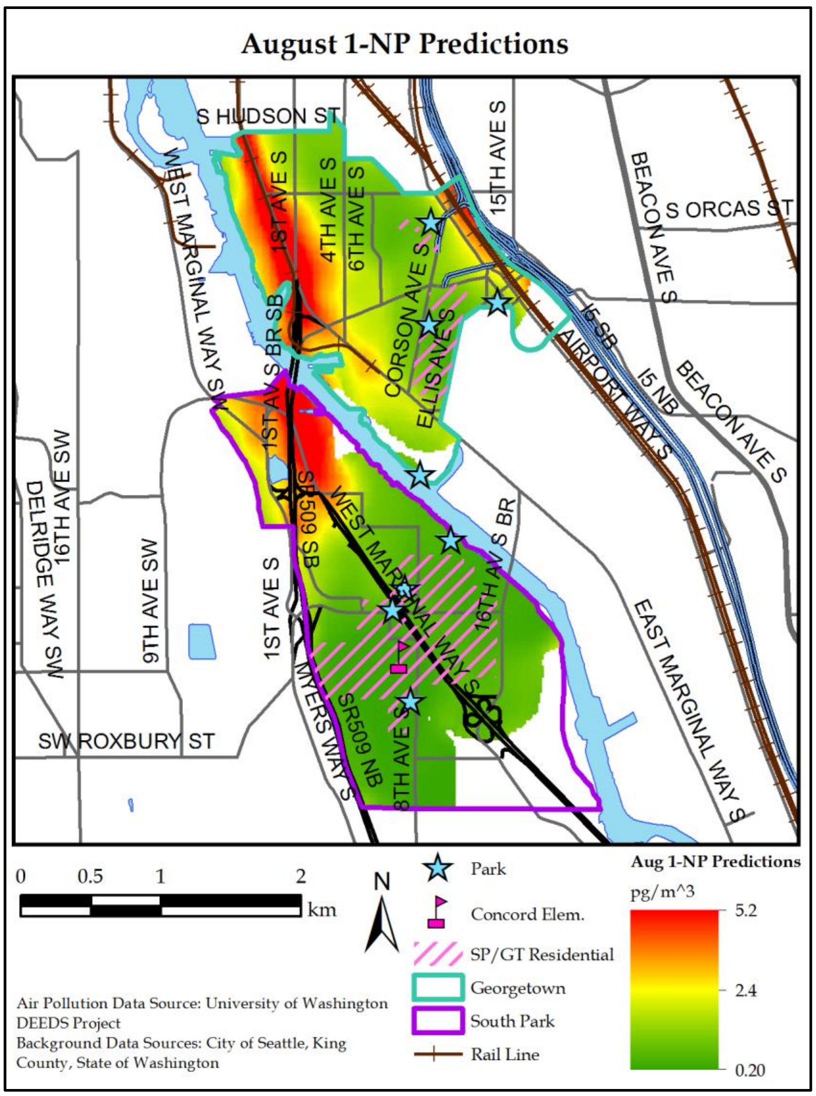

Figure 1. Map of August 1-NP prediction gradient

In addition to models of individual pollutants, models were also generated for a continuous pollution score, which represents a linear combination of standardized levels of 1-NP, BC and NO_x. The August pollution score model had the highest cross-validated R^2 of the prediction models (0.89).

By combining community-based monitoring and advanced modeling approaches, this study was able to identify and display predictors of fine-scale differences in concentrations of diesel exhaust pollution in the communities of South Park and Georgetown. Pollution levels were generally higher in South Park and Georgetown than comparison sites in other residential neighborhoods (Queen Anne and Beacon Hill). Within South Park and Georgetown, levels were highest in areas of heavy traffic and industrial activity.

BACKGROUND

INTRODUCTION

Seattle's South Park and Georgetown neighborhoods are located a short distance from the Port of Seattle and contain a large network of commercial traffic corridors. The high volume of diesel trucks in these neighborhoods prompted concern among community members about exposure to ambient diesel exhaust. In a 2009 survey by Puget Sound Sage, a Seattle-based community organizing coalition, 60% of residents surveyed in a convenience sample responded that they believed pollution from commercial trucks affected the health of their family (Puget Sound Sage, 2009). In response to these concerns, the University of Washington partnered with Puget Sound Sage to conduct the Diesel Exhaust Exposure in the Duwamish Study (DEEDS). This study sought to characterize the gradient of diesel exhaust markers across the South Park and Georgetown neighborhoods and identify fine-scale spatial variations in diesel exhaust levels.

SPECIFIC AIMS

The specific aims of this study are:

1. Implement a high-density air sampling campaign in South Park and Georgetown to measure several markers of diesel exhaust: 1-nitropyrene (1-NP), black carbon (BC), oxides of nitrogen (NO_x) and fine particulate matter ($PM_{2.5}$).
2. Develop prediction models of 1-NP, BC, NO_x and a combined pollution score in order to identify the predominant spatial features that predict levels of diesel pollution.
3. Generate maps of the gradient of diesel exhaust markers at the neighborhood scale using selected model covariates.

DUWAMISH VALLEY NEIGHBORHOODS

South Park and Georgetown are located south of downtown and the Port of Seattle along the Duwamish River (see Figure 1).

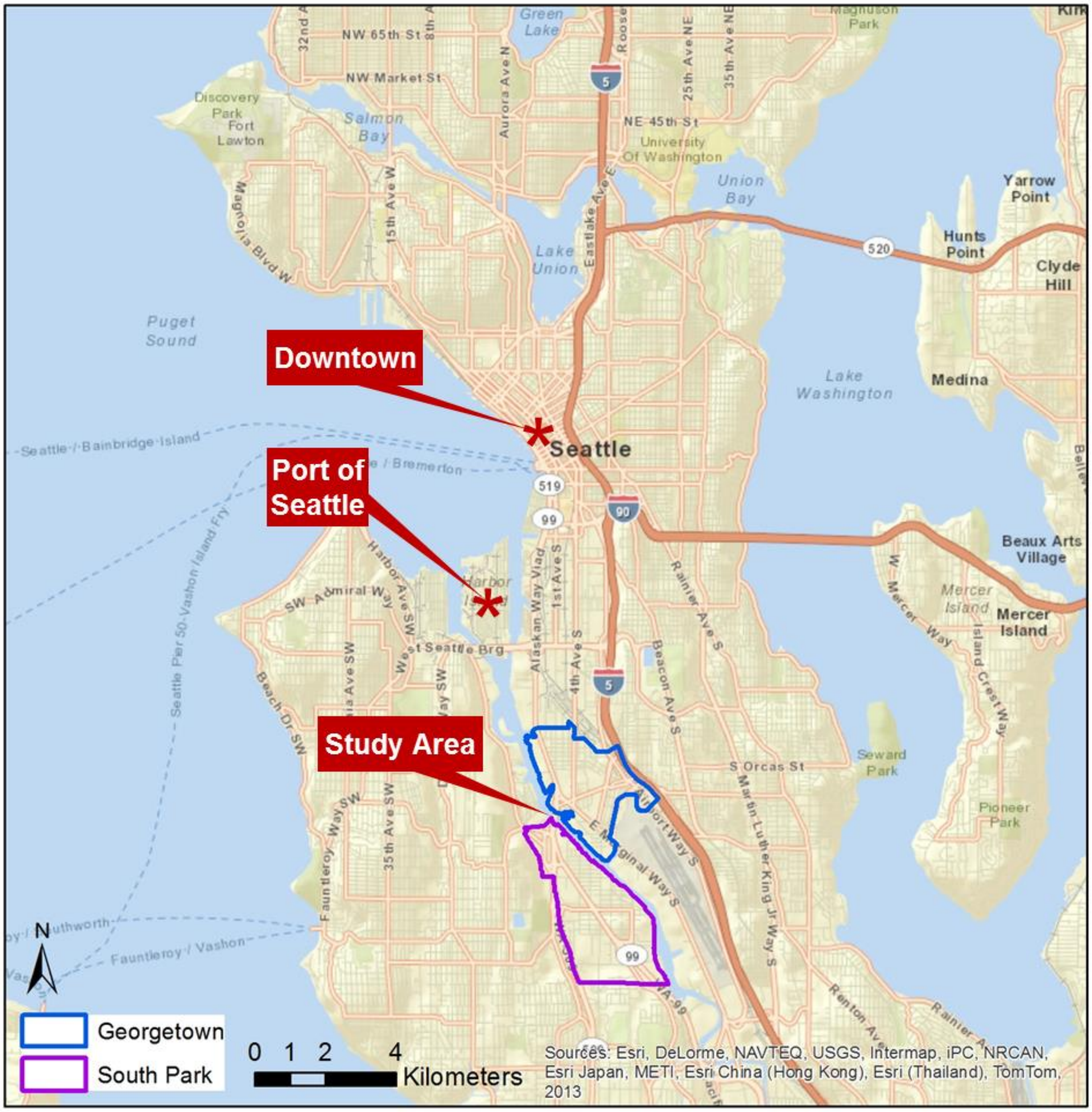

Figure 2. Overview map of study area

Commercial traffic routes serving these neighborhoods include Interstate 5, Washington State Routes 99 and 509, and a number of arterial roads. Because of this dense network of commercial traffic corridors, the Duwamish Valley neighborhoods are a key thoroughfare for commercial traffic between the Port of Seattle and points across the Pacific Northwest. Over 10 trucking companies are headquartered in South Park and Georgetown, and associated trucks typically access these facilities several times a day. Several other sources of ambient air pollution are located within and around South Park and Georgetown. These include an 11-acre Waste Management transfer station, a major First Student school bus depot that houses approximately 200 buses, commercial and passenger rail lines, Seattle's primary industrial zone, and the King County Airport (see Figure 2).

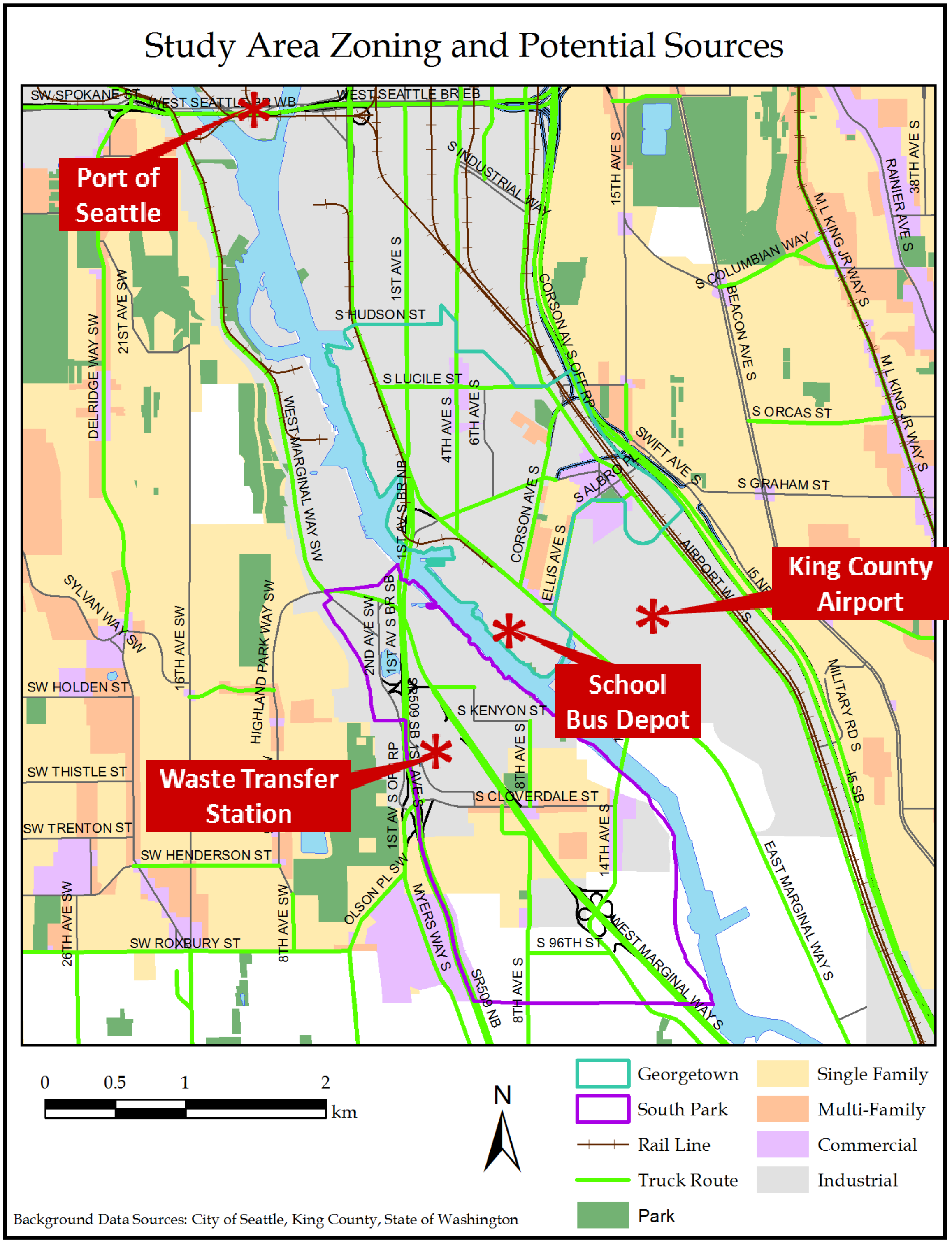

Figure 3. Duwamish Valley zoning and potential sources

The total area of the South Park and Georgetown neighborhoods is 2.8 square miles or 7.2 square kilometers. Approximately 73% of this area is zoned for industrial use, 6% for commercial use and 20% for residential use. As of the 2010 census, the combined population in both neighborhoods was approximately 5,800 people (King County, 2012).

Previous Research

Diesel exhaust exposure is a health concern in these neighborhoods because of its association with a number of adverse health outcomes. Diesel engine exhaust was reclassified by the International Agency for Research on Cancer (IARC, 2012) as carcinogenic to humans (Group 1) in 2012. Epidemiological studies have shown an elevated risk of lung cancer associated with long-term diesel exhaust exposure in occupationally exposed populations (Silverman et al., 2012; Attfield et al., 2012; Olsson et al., 2011; Garshick et al., 2008). Acute effects of diesel exhaust exposure include respiratory irritation and inflammation (Hesterberg et al., 2009; Sydbom et al., 2001; Nordenhäll et al., 2000; Nightingale et al., 2000). Traffic-related air pollution, comprised of both diesel exhaust and gasoline exhaust, has also been found to lead to both onset and exacerbation of asthma in children (Gent et al., 2009; McConnell et al., 2010).

Two recent studies in south Seattle have identified diesel exhaust exposure as a predominant environmental health risk for residents in the area. In response to a petition by south Seattle residents, the Washington State Department of Health conducted an air toxics health assessment based on risk estimates in the Duwamish Valley in 2008. This assessment found that the increased cancer risk attributed to diesel exhaust exposure in these neighborhoods was three times that attributed to gasoline exhaust (Palcisko, 2008). The emissions estimates used in the health assessment were modeled from estimated traffic counts on highways and interstates. They did not involve direct measurement of pollutants or account for truck traffic on non-highway roads.

In 2010, the Puget Sound Clean Air Agency conducted an air toxics evaluation in partnership with the University of Washington to characterize the health risks of exposure to air toxics in the Duwamish Valley and other area neighborhoods. This risk assessment was based on direct measurement of over 100 pollutants, including several markers of diesel exhaust. Two of the sampling sites were located in the Duwamish Valley. The study estimated that diesel exhaust exposure accounted for over 70% of the elevated cancer risk of the air toxics measured for residents of the Duwamish Valley (Gilroy, Strange & Yost, 2010).

These previous studies highlight the health concerns associated with diesel exhaust exposure in South Park and Georgetown and the need for further information about the gradient of diesel exhaust within these individual neighborhoods. The DEEDS project sought to expand upon the existing body of knowledge by modeling the spatial distribution of diesel exhaust markers at a fine scale using measurements from a high-density air sampling campaign.

POLLUTANTS MEASURED

Four pollutants (1-NP, BC, NO_x and $PM_{2.5}$) were selected for sampling. These markers of pollution vary in their specificity to diesel sources. The most diesel-specific pollutant measured was 1-nitropyrene, a particle-associated nitrated polycyclic aromatic hydrocarbon (nitro-PAH). 1-NP is a byproduct of combustion and the most prevalent nitro-PAH found in diesel engine exhaust. It is classified by the International Agency for Research on Cancer (IARC, 1985) as possibly carcinogenic to humans (Group 2B). Though 1-NP has historically been detected in other sources, including airplane exhaust and coal combustion fly ash (Chan, 1996), Hayakawa *et al.* (1995) found that ambient 1-NP concentrations were highly correlated with traffic volumes (r=0.93). As a central goal of the DEEDS project was to characterize diesel exhaust as distinct from gasoline engine exhaust, 1-NP was a suitable pollutant to measure because it is only detectable in trace amounts in gasoline exhaust and other sources. In a study of 1-nitropyrene concentrations in lab-generated diesel and gasoline engine exhaust, Hayakawa *et al*. (1992) determined that 1-nitropyrene concentrations were over 200 times as high in diesel engine particles relative to gasoline engine particles. Previous research indicates that 1-NP is decomposed in the presence of ultraviolet light (García-Berríos & Arce, 2012; van den Braken—van Leersum *et al.*, 2010), and thus some atmospheric photodegradation of 1-NP can be expected prior to deposition, particularly during sunny weather. Neither extensive 1-NP field sampling campaigns nor spatial models of 1-NP have been described in the literature to date.

Black carbon is a general term for carbonaceous aerosols that reflect and absorb visible light. In this research it was measured at active sites as the absorption coefficient of particles in units of m^{-1} (Bond, Anderson, & Campbell, 1999) and via an Aethalometer® as particle concentration in units of $\mu g/m^3$. A previous study of diesel exhaust markers in Harlem by Kinney *et al.* (2000) found that particle absorption coefficient and elemental carbon mass concentration were highly correlated, with r=0.95. Elemental carbon is frequently used as a surrogate for diesel exhaust, though other sources include wood combustion and, to a lesser extent, gasoline exhaust. The contribution of diesel exhaust to fine particle elemental carbon as estimated by 11 source apportionment studies reviewed by Schauer (2003) using National Institute for Occupational Safety and Health (NIOSH) methods ranged from 57% - 96%, with a median of 86%.

Oxides of nitrogen (NO_x) are primarily composed of nitrogen dioxide (NO_2) and nitric oxide (NO). These gases are formed from combustion of fossil fuels, including diesel, and are frequently used as a marker of traffic-related pollution in studies of air pollution (Mercer et al., 2011; Wilton et al., 2010; Eckel et al., 2011). Though less specific to diesel exhaust than 1-NP, NO_x is relatively easy and inexpensive to sample, and the samplers do not require the use of electricity. Sampling for NO_x was feasible at a much higher density and across a broader geographic area in the Duwamish Valley than was sampling for 1-NP and BC.

Fine particles ($PM_{2.5}$) are particles with diameters of 2.5 µm or less, and this fraction of particles primarily includes combustion particles and smog. Combustion sources of particles in urban settings typically include gasoline exhaust, industrial sources and wood smoke, and $PM_{2.5}$ is therefore not a specific marker of diesel exhaust. However, $PM_{2.5}$ is a commonly measured component of air pollution that is currently regulated by the U.S. Environmental Protection Agency (EPA). Due to the multiple sources of ambient $PM_{2.5}$, emission densities in urban areas are more uniform (Burton et al. 1996), and therefore $PM_{2.5}$ measurements are not expected to vary widely at the neighborhood scale.

METHODS

SAMPLING SITE SELECTION

Active Sampling

Active sampling for 1-NP, BC and $PM_{2.5}$ was conducted simultaneously at 23 outdoor sites in both August and December. One additional site was sampled in each season, for a total of 24 data points per season. Of these 24 sites, 19 were located in the study area and 5 were located in other neighborhoods to serve as comparison sites. Four of these comparison sites (the Queen Anne, Beacon Hill, and downtown agency monitors, and the King County Airport) were excluded from the spatial models due to their distance from the study neighborhoods. The remaining 20 sites will be referred to as the "core study area." The density of sites within the South Park and Georgetown neighborhoods was approximately 7 sites per square mile.

Table 1. Number of sampling sites by neighborhood

	South Park	Georgetown	Other Neighborhoods	Total	Included in Modeling
August	12	7	5	24	20
December	11	8	5	24	20

The majority of sampling sites were at homes, though sampling was also conducted at 4 businesses and 8-9 public sites. Public sites included 4 monitoring sites operated by public agencies (the Puget Sound Clean Air Agency and the Washington

Department of Ecology) in the Queen Anne, Beacon Hill, downtown Seattle and SoDo (South of Downtown) neighborhoods. Other public sites sampled were the South Park Neighborhood Center (August only), the South Park Community Center, the Georgetown campus of South Seattle Community College, and the King County Airport (see Figure 4). Locations of home and business sites have been generalized to the nearest intersection to protect participant privacy in all maps appearing in this report.

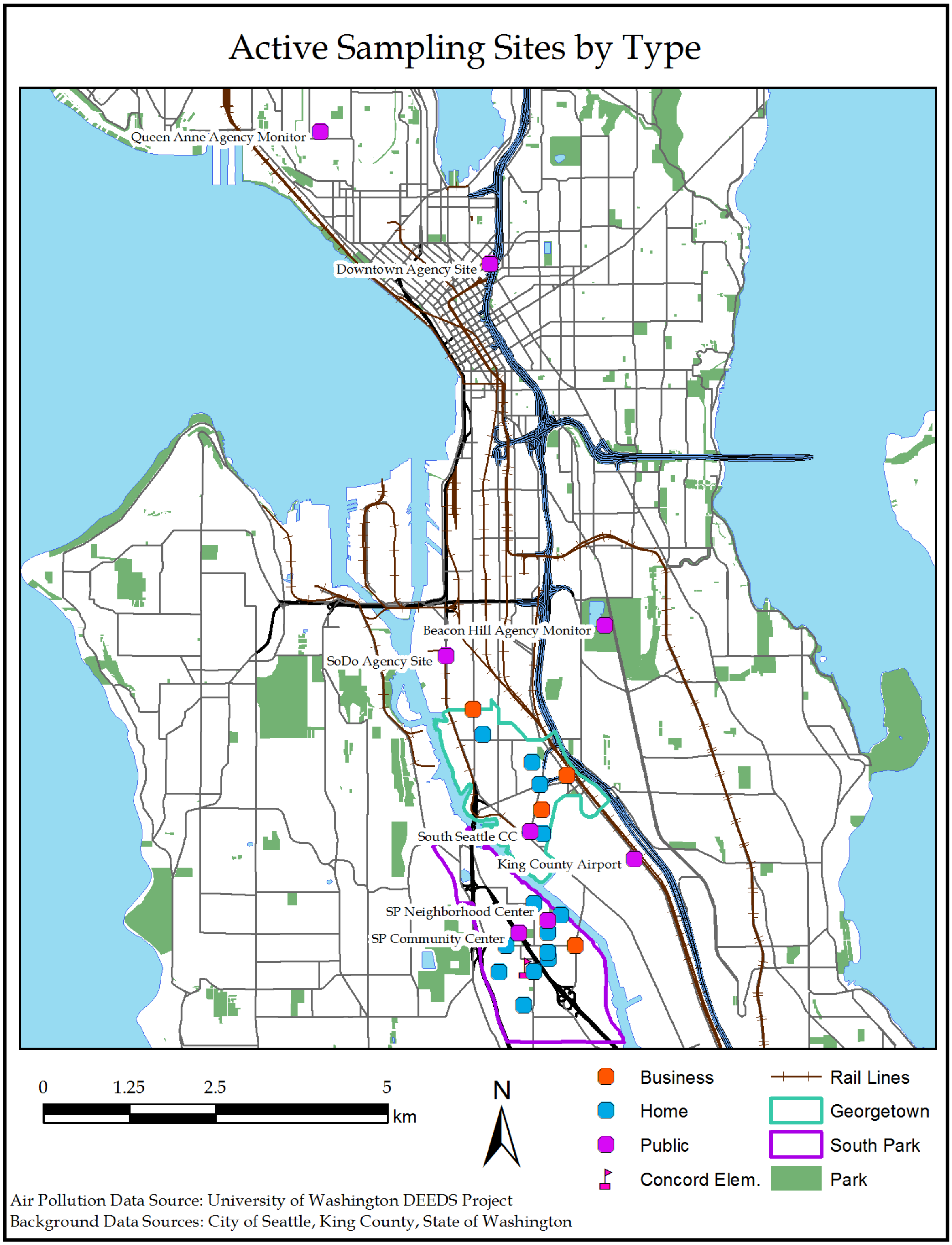

Figure 4. Map of active sampling sites by type. Home/business sites were generalized to the nearest intersection.

Feedback from community members guided the selection of sampling sites. In spring 2012, Puget Sound Sage surveyed approximately 550 members of the South Park and Georgetown communities who either lived or worked in the study area at the time. The majority of respondents identified commercial trucks as their top diesel exhaust source of concern and residential areas as their priority locations to monitor. Sampling sites were selected to maximize coverage in residential areas in accordance with these responses. Of the 19 sites within the Duwamish Valley, 12 were located in residential zones in August and 11 in December (see Figure 5).

In addition, sites were selected at a wide range of distances from commercial truck routes to increase the likelihood that statistical models would be able to discern the impacts of commercial trucking. Before sites were selected, the study area was divided into 18 geographic zones. Zone boundaries were drawn to maximize variation in distance to truck route between zones and minimize this variation within zones. Puget Sound Sage recruited a minimum two volunteers per zone who were interested in hosting a monitor at their home or business. The research team visited each home or business to screen for sampling site locations. The most suitable site in each zone was selected based on the security of the location, the availability of canopy-free space away from walls or fences, and the proximity of outdoor electrical outlets.

Table 2. Zoning designation of sampling sites within core study area

	Residential	Commercial	Industrial
August	13	2	4
December	12	2	5

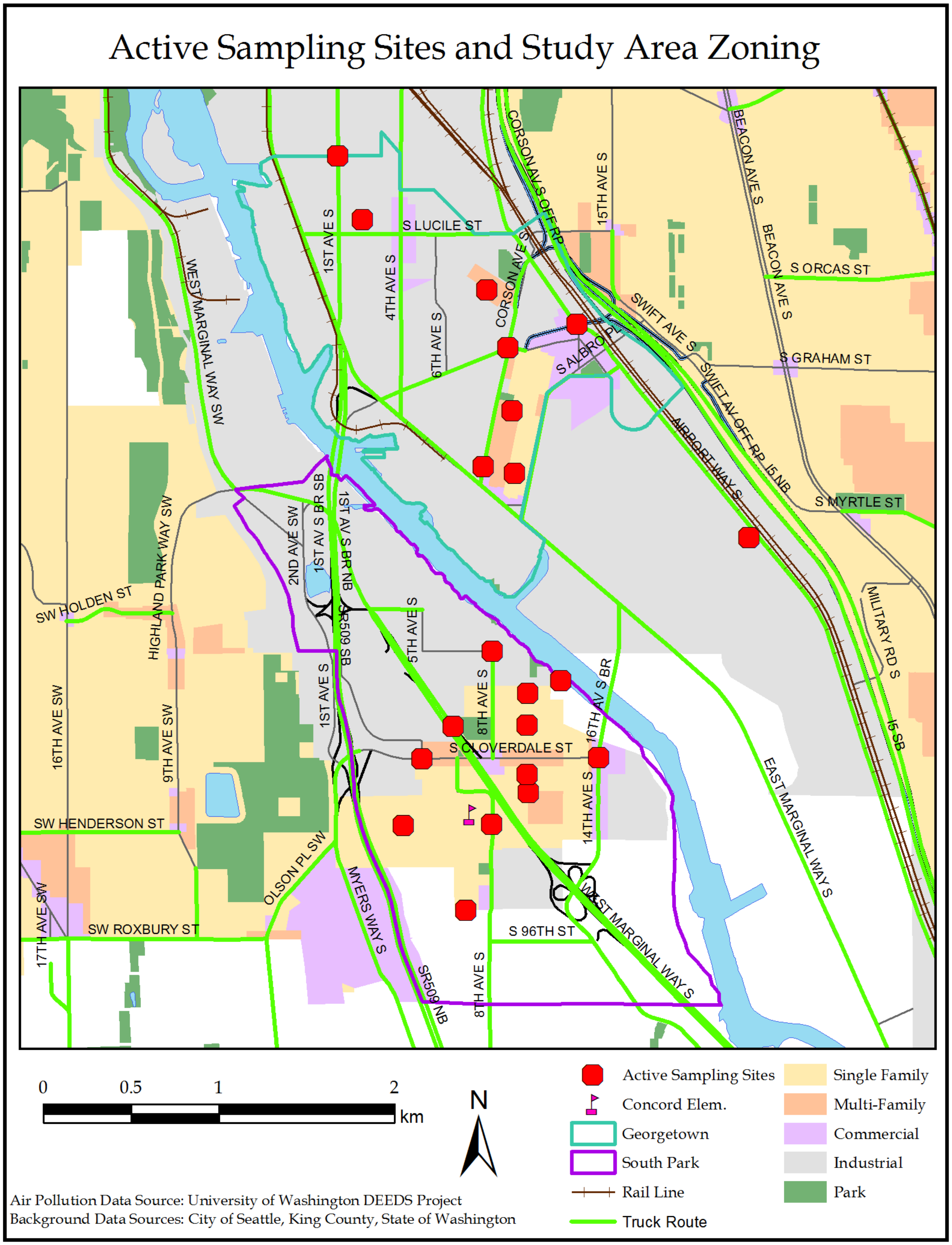

Figure 5. Map of Duwamish Valley active sampling sites and zoning. Home/business sites were generalized to the nearest intersection.

Monitors were located either in yards or on rooftops. Sites in back or front yards were located at least 6 feet away from walls or fences and outside of canopy cover. Residents were asked to record any barbecuing, lawn mowing or idling of personal vehicles that took place in the vicinity of the monitor and to avoid these activities if possible. Rooftop sites were located at least 6 feet away from roof edges (see Figure 5). Two monitors (one business and one public site) were flagged as atypical set-ups because they were suspended from the edge of a roof; this public site was only sampled in August.

Figure 6. Typical 2nd-story rooftop sampler

Passive Sampling

Sampling for NO_x was conducted at all active site locations. NO_x samplers were attached to active sampling site setups at a height of approximately 5 feet (see Figure 6). Additional NO_x samplers were suspended from utility poles located throughout the South Park and Georgetown neighborhoods and at comparison sites in Beacon Hill, SoDo, downtown and Delridge. Utility pole samplers were attached at a height of 8 feet from the ground facing away from the street with approval from Seattle City Light (see Figure 7).

Figure 7. Typical NOx sampler on utility pole

NO$_x$ sampling was conducted at 74 utility pole sites in August and 75 in December, for a total of 99 sites in each season. Utility pole sites were selected for several different purposes. Some were chosen to provide sampling coverage in geographic areas where no suitable active sampling locations were found. Others were grouped at different distances from expected sources, such as busy intersections and highway interchanges, to provide information on dispersion patterns away from traffic sources. Others were placed in areas of lower expected concentrations, such as parks and hilltops in comparison neighborhoods, to provide sufficient contrast in measurement results. All utility pole sites were included in NO_x models with the exception of the Queen Anne agency site. A map of all NO_x sampling locations, including both active sampling sites and utility pole sites, is shown in Figure 8 and a close-up of NO_x sampling sites in South Park and Georgetown is shown in Figure 9.

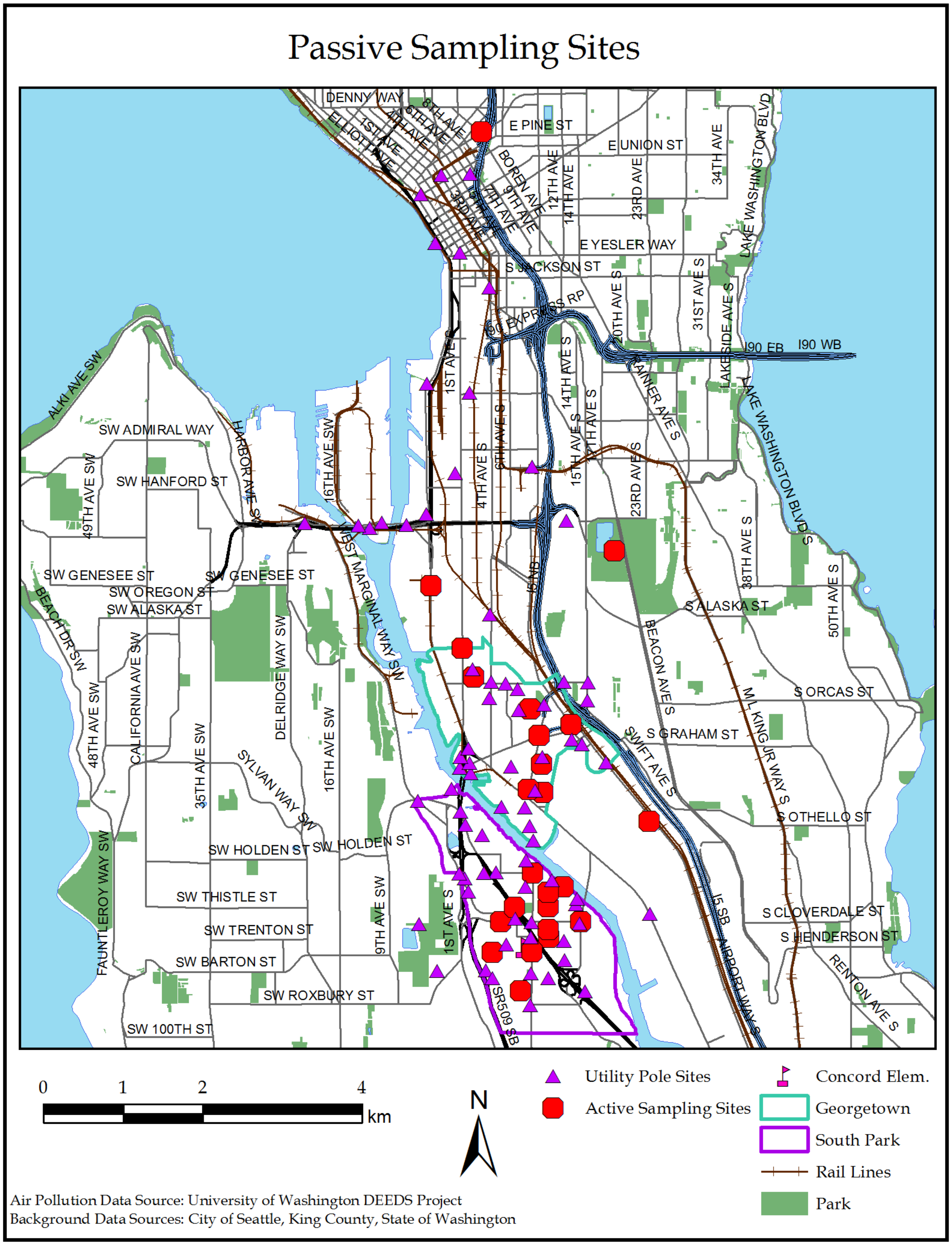

Figure 8. Map of all passive sampling sites. Home/business sites were generalized to the nearest intersection.

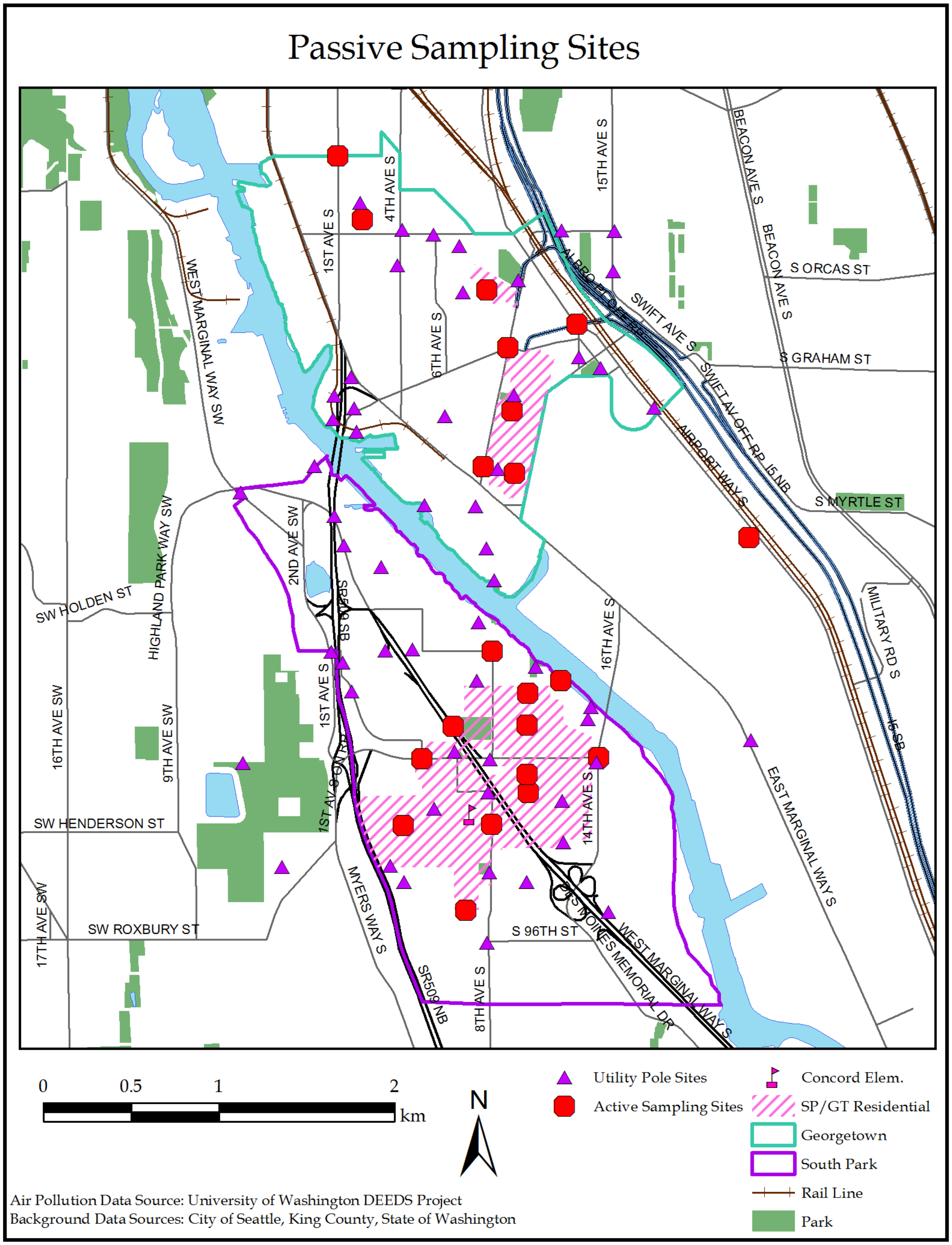

Figure 9. Close-up map of passive sampling sites in South Park and Georgetown. Home/business sites were generalized to the nearest intersection.

SAMPLING PROTOCOL

Sampling was conducted August 18-30 (12 days) and December 1-14 (13 days), 2012. Particles were collected on 37mm Teflon filters (Pall Life Sciences, Port Washington, NY) loaded in Harvard Personal Exposure Monitors (HPEMs, Harvard School of Public Health, Boston, MA) with a 50% cut point of 2.5µm. At each active sampling site, two HPEMs were suspended beneath waterproof rain caps at a height of approximately 5 feet from the ground or rooftop. Sampling pumps (Medo USA Inc., Hanover Park, IL) operated at approximately 1.8 L/min and were equipped with dual valve timers to direct airflow through each HPEM 50% of the time in alternating 5-minute periods.

Continuous sampling flow rates were measured in the field using rotameters (Cole Parmer, Inc., Vernon Hills, IL) that were calibrated against a primary flow meter during the August sampling period. Flow rates were adjusted to within 3% of the 1.8L/min target flow at the onset of sampling and at a mid-sampling check roughly halfway (5-7 days) into the sampling period. The total air volume per sample (*V*) was calculated using Equation 1:

$$V(m^3) = \frac{\left(\frac{flow_a + flow_b}{2} * time_1\right) + \left(\frac{flow_c + flow_d}{2} * time_2\right)}{2}$$

Equation 1. Calculation of total airflow per sample

Where $flow_a$ = initial flow (m^3/minute)

$flow_b$ = mid-sampling check flow (m^3/minute)

$flow_c$ = mid-sampling check adjusted flow (m^3/minute)

$flow_d$ = final flow (m^3/minute)

$time_1$ = length of first half of sampling period (minutes)

$time_2$ = length of second half of sampling period (minutes)

The lapsed times between sampling onset and the mid-sampling check ($time_1$) and between the mid-sampling check and the end of the sampling period ($time_2$) were calculated from log sheets completed by field staff. The total airflow was divided by 2 to account for the 50% timers.

NO_x was sampled using Ogawa sampling badges, which consist of a plastic cylindrical barrel containing a NO_2 collection pad on one end and a NO_x collection pad on the other end. Ambient NO_2 and NO_x were absorbed onto these collection pads through holes in diffuser end caps (Ogawa, 2006). Average 2-week concentrations of NO_2 were calculated from the mass collected on coated filters according to Equation 2 (Ogawa, 2006):

$$NO_2(ppb) = \frac{NO_2(\mu g) * \alpha * 1000}{t}$$

Equation 2. Calculation of NO_2 mole fraction in ppb

Where t = total lapsed minutes of sampling

α = a constant based on average temperature, pressure and relative humidity during each sampling period

Total NO mass was calculated from the difference in NO_x and NO_2 mass collected on each sampler. Average two-week concentrations of NO were calculated using equation 2, with mass and α values specific to NO. Average 2-week concentrations of NO_x were calculated as the sum of NO and NO_2 concentrations.

Lab Analysis

1-Nitropyrene

Collected particles were analyzed for 1-nitropyrene content according to a previously reported method (Miller-Schulze, 2010). In brief, samples were spiked with an isotopically labeled internal standard, extracted in solvent, evaporated, and then resuspended in a solution of ethanol, sodium acetate and acetic acid. The suspension was filtered prior to analysis via high-performance liquid chromatography tandem mass spectrometry (HPLC-MS/MS). 1-NP results are reported as a mass concentration in units pg/m^3.

Fine Particulate Matter ($PM_{2.5}$)

The 1-NP sample loading was determined using the fine particulate matter ($PM_{2.5}$) mass concentration of the Teflon filter samples. $PM_{2.5}$ mass concentration was assessed by gravimetric analysis with a Mettler Toledo UMT-2 microbalance in a temperature- and humidity- controlled environment (Allen et al., 2001) using standard filter weighing procedures (U.S. EPA, 1998).

Black Carbon (Active Site Measurements)

Black carbon is a measure of the blackness of the particles and is quantified by measuring filter reflectance both before and after sampling. Reflectance was assessed using a Smokestain Reflectometer (Diffusion Systems Ltd Model 43D, London, United Kingdom) as described in Dotse, Asane and Ofosu (2012). Absorption coefficients (σ_{ap}) of collected particles in units m^{-1} were calculated from Equation 2:

$$\sigma_{ap}(m^{-1}) = \left(\frac{A}{2V}\right) * \ln\left(\frac{\overline{R_b}}{R_s}\right)$$

Equation 3. Absorption coefficient equation

Where A = area of the exposed filter (0.000730246 m^2)

V = sample volume (m^3) (see Equation 1)

$\overline{R_b}$ = average change in reflectance of field blanks

R_s = change in reflectance of sample filter

Oxides of Nitrogen

Ogawa passive samplers (Ogawa & Company USA, Pompano Beach, FL) were used to measure NO_2 and NO_x; these were processed and analyzed in the Environmental Health Laboratories at the University of Washington. Ion chromatography (IC) was used to analyze the sample extracts for nitrite and nitrate for the quantification of NO_2. The IC system consisted of a Dionex ICS1000 with an AS40 autosampler and conductivity detector (Dionex, Sunnyvale, CA). A Dionex IonPac AS9-HC analytical column and AG9-HC guard column were used along with an ASRS-ULTRA-II suppressor run in recycle mode at a current of between 37 and 45mA. A 25 μL sample loop was used with a 9mM sodium carbonate eluent, set to a flow rate of between 0.75 and 1.0 mL/min.

Ultraviolet spectroscopy (UV) was used for analysis of NO_x. A Molecular Devices Spectromax 190 absorbance microplate reader (Molecular Devices Corp., Sunnyvale, CA) was employed for the UV spectroscopy method. Nitrite ions were detected colorimetrically at a wavelength of 545 nm and the instrument was calibrated during each analysis session using nitrite ion standards.

POLLUTION SCORE

The 1-NP, BC and NO_x measurement results were synthesized into August and December "pollution scores" at each active sampling site using singular value decomposition (SVD). $PM_{2.5}$ results were excluded from the pollution score for two reasons. First, of the pollutants measured, $PM_{2.5}$ is the least specific to diesel sources. Second, $PM_{2.5}$ results were relatively homogenous across the study area, and the magnitude of the observed variations was considered to be within the margin of error of the analysis method.

SVD is a matrix factorization technique for reducing the dimensions of a dataset while maintaining the level of variability found in the original data (c.f. Golub & Reinsch, 1970). Within each season, levels of each pollutant were first log-transformed and standardized. The pollution score was then calculated as the weighted sum of each standardized pollutant value with weights derived from the SVD method. Since the pollutants were highly correlated in general, the weights were comparable and ranged from 0.56 – 0.58 in August and from 0.56 – 0.59 in December. Therefore, the contributions of each pollutant to the pollution score were roughly equivalent, and the pollution score can be considered an approximation of the relative magnitude of pollutant values at each site. Prediction models were then built for the pollution score in each season.

QUALITY ASSURANCE AND CONTROL

In each season, at least 5 lab blank and 6 field blank HPEMs (one of each for every 10 sample filters) were assembled to identify any contamination issues in the lab or field. Ten lab blank and 10 field blank Ogawa badges were assembled as well. Lab blanks were immediately placed in sealed plastic bags upon assembly and stored in the laboratory throughout the sampling period. Field blank HPEMs and Ogawa badges were also stored in plastic bags, and each field technician carried at least one field blank with them on the first day of each sampling campaign. The field blanks were removed from plastic bags for approximately 5 seconds at a sampling site of the technician's choosing, then resealed and stored. This process was repeated on the final day of sampling only during the August sampling period. Field blanks were stored in the laboratory during the remainder of the sampling period.

Both lab and field blank filters were analyzed for 1-NP and BC. The average 1-NP mass on blank filters was less than 3% of the average mass on sample filters in both seasons, indicating that significant lab or field contamination of filters was unlikely. The change in reflectance values of the field blank filters, which was within the margin of error of the reflectometer, was used to adjust the absorption coefficient results as shown in Equation 2.

Equivalent volumes of air were sampled by "pump duplicate" HPEMs operated by a single pump at each site. "Site duplicate" filters were also collected by side-by-side duplicate setups installed at two sampling sites. Every filter was analyzed for BC. The average percent error in absorption coefficient between pump duplicates was 16% in August and 7.4% in December, calculated as the ratio of the difference in σ_{ap} to the average of the two σ_{ap} values. The average percent error in σ_{ap} between site duplicates was 10% in August and 8.6% in December. Final BC results by site were calculated as the mean of pump and site duplicate filters collected at each site.

Only one filter per site was analyzed for 1-nitropyrene, with the exception of 2 duplicates in August and 5 duplicates in December. The average percent error in 1-NP concentration among these duplicates was 11% in August and 14% in December. Six analytical replicates from the August sampling period were selected for reanalysis with the December filters in order to compare the measurement precision between batches. The average percent error among the analytical replicates was 40%. Average percent error was calculated as the ratio of the largest difference among any pair of replicate filters to the average concentration of all replicate filters. Based on this high level of error in replicates between batches, pollutants were modeled separately in each season and were first standardized within each season when combined into multi-season models. Final 1-NP concentrations by site were calculated as the average of only the duplicates analyzed in the same batch. August results were not adjusted for the analytical replicates analyzed in December because of the poor between-batch precision.

The average percent error in NO_x concentration between duplicates in August and December was 5.5% and 12%, respectively, calculated as the ratio of the difference between duplicate concentrations to the average of the two duplicate concentrations. August and December samples were analyzed in separate batches. Prior to conversion into concentration units, August NO_x was corrected by subtracting the average field and laboratory blank analyte mass and December NO_x was corrected by subtracting the average laboratory blank analyte mass. Seven of the December NO_x samples were greater than the highest calibration standard, though there was no reason to suspect that the data of these estimates is invalid. All NO_x concentrations were above the limit of detection.

STATISTICAL METHODS

Land-use regression (LUR) was used to develop spatial models of the two pollutants. LUR is a multiple linear regression technique that uses measured levels of a pollutant as the dependent variable and spatial covariates such as land use and road density as independent variables. Spatial covariates can then be used to predict pollutant levels in locations without measurements (Jerrett et al., 2005). LUR has been used to predict levels of traffic-related pollutants in urban environments in several previous studies and is a well-established method of air pollution modeling (Hoek et al., 2008; Ryan & LeMasters, 2007).

Previous studies using LUR have generally modeled traffic-related pollutants over broader geographic areas than the DEEDS effort. Models of NO_x and/or NO_2 have been described at the neighborhood scale (Mavko, Tang and George, 2008), the citywide scale (Wilton et al., 2010; Mercer et al., 2011; Briggs et al., 1997; Gonzalez et al., 2005) and the national scale (Sampson et al., 2013; Novotny et al., 2011). Previous studies have also built LUR models of $PM_{2.5}$ and light absorbing or elemental carbon at the citywide scale (Larson et al., 2009; Clougherty et al., 2008; Ryan et al., 2008; Henderson et al., 2007; Ross et al., 2007). While application of LUR at the sub-neighborhood scale is unique, it has been used successfully to predict a fine-scale NO_2 gradient (Mavko et al., 2008). The DEEDS modeling approach differs from most previous studies in its small geographic scale, high density of sampling data points, and novel use of a diesel-specific pollutant (1-NP). Measurement results of all pollutants were log-transformed prior to modeling because the data were log-normally distributed.

Mobile-source pollution estimates from both dispersion modeling and direct-reading instruments were included as covariates to create hybrid land-use regression/dispersion models. The hybrid model was first developed by Wilton *et al.* (2010), who found that inclusion of line source dispersion model predictions enhanced the predictive ability of a LUR model of NO_x in Seattle and Los Angeles. Hybrid models have also been described by Lindstrom *et al.* (2013). The additional inclusion of on-road emissions estimates from direct-reading instruments as model covariates has not been described in the literature to date.

DISPERSION MODELING

Mobile-source pollution estimates were generated using the CAL3QHCR dispersion model (U.S. EPA, 1995). This model predicts concentrations of a non-reactive pollutant at receptor sites using a Gaussian dispersion equation. Specific pollution estimates were generated for the 12-13 days of each sampling period based on roadway locations, estimates of traffic volumes and meteorological data. Traffic inputs were derived from the Travel Demand Model Version 1C developed by the Puget Sound Regional Council (PSRC, 2008). This model contains car and truck volume forecasts on each segment of highway and major arterial road in the study area, based on commuter surveys and a sample of empirical traffic counts. Diurnal pattern data were obtained from the University of Washington Smart Transportation Applications and Research (STAR) Lab. Meteorological data were obtained from the National Weather Service station at the King County Airport with the exception of mixing height, which was obtained from the Seattle-Tacoma International Airport.

MOBILE MONITORING

Additional on-road emissions data were collected using a dual-channel Aethalometer® (microAeth® Model AE52, Magee Scientific, Berkeley, CA). The instrument's inlet was affixed to a hybrid vehicle that drove a fixed route throughout the study area 5-6 times per day (see Figure 6). This route included 4 loops per trip of 4 consecutive right turns around 11 of our sampling sites. Mobile monitoring was conducted on 6 days in September 2012 and 6 days in December 2012. The December mobile monitoring campaign was concurrent with the December air sampling campaign, but September was the earliest the mobile platform was available following the August sampling period. In each season, 5 monitoring days were weekdays and 1 was a weekend day. All mobile monitoring took place during the hours of 2pm to 7pm to capture peak traffic during the evening rush hour. A total of 11,561 data points were collected within the South Park and Georgetown neighborhoods.

As aerosols collected on a filter, the instrument continuously measured the change in rate of absorption of transmitted light at the 880 nm and 370 nm wavelengths. The 880 nm channel indicates the presence of black carbon (BC), and the 370 nm channel (UV) indicates the presence of both black carbon and additional aromatic organic compounds, both in units of $\mu g/m^3$ (Magee Scientific, 2010). The log-transformed concentrations from the BC and UV channels on all 12 sampling days were averaged within buffers of 300 meters and 500 meters around each sampling site and included as model covariates.

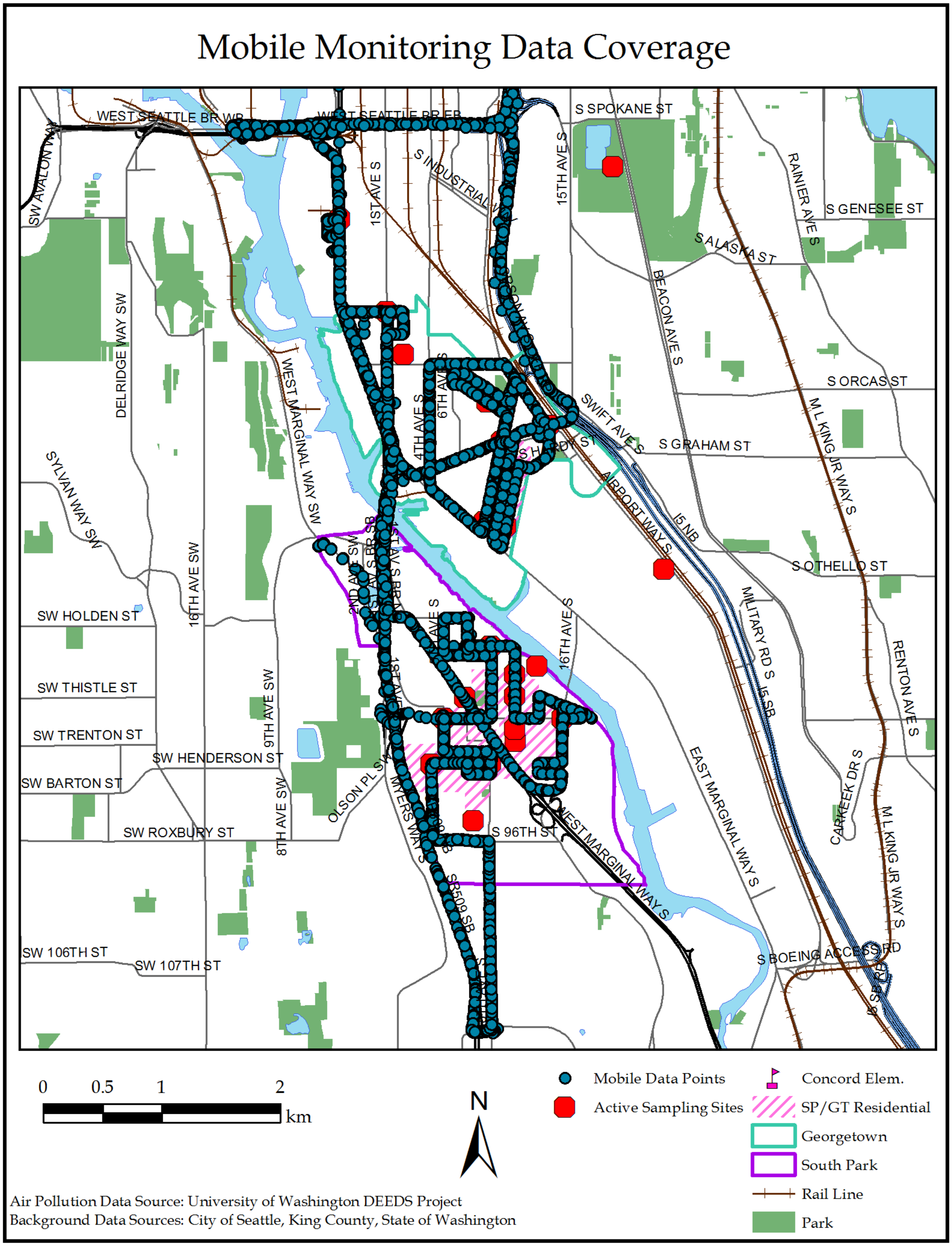

Figure 10. Mobile monitoring data coverage. Home/business sites were generalized to the nearest intersection.

SPATIAL COVARIATES

Geographic attributes of the sampling sites, including land use, road density, and population, were extracted using Tele Atlas (TomTom, Amsterdam, Netherlands) and ArcGIS 10.1 (ESRI, Redlands, CA). Spatial data were obtained from the following sources: National Emissions Inventory (U.S. Environmental Protection Agency), Tele Atlas, Google Maps, U.S. Census Bureau, Multi-Resolution Land Characteristics Consortium 2006 National Landcover Dataset (U.S. Geological Survey), National Geospatial Intelligence Agency, and the Bureau of Transportation Statistics. The 107 spatial variables initially considered for the models are summarized in Table 3.

Table 3. Spatial covariates considered for modeling

Variable	Type	Buffer Radius	Description
log10.m.to.<type>	a1, airp, coast, port, ry, rr, truck, road, intersect, interchange12, interchange3	N/A	Log_{10} meters to A1 road, airport, coast, port, rail yard, railroad, truck route, road, intersection, A1 and A2 road interchange, A3 road interchange
ll.a1/a23.<buffer>	N/A	100m, 150m, 300m, 500m, 750m, 1500m	Length of A1 and A2/A3 roads in various buffer distances
intersect.<buffer>	N/A	500m, 1000m	Intersections in various buffer distances
pop.s01000	N/A	1000m	Population in 1000m
log10.pop. <buffer>	N/A	500m, 1000m, 1500m, 2500m	Log_{10} population in various buffer distances
interchange <type>.<buffer>	a12, a3	500m, 1000m	Interchanges with A1 roads by road type in various buffer distances
imp.<buffer>	N/A	50m, 150m, 300m	Impervious surface in various buffer distances
elev.elevation	N/A	N/A	Elevation
rlu/rlc.dev.<type>. <buffer>	open, openlow, medhi, hi	50m, 150m, 300m, 750m, 1000m, 3000m	Intensity of development (low, medium-high, high) in various buffer distances
rlc.<type>. <buffer>	anyforest, anyflat, openbasic, openplus	150m, 300m, 750m, 1000m, 3000m	Land characteristics (e.g. forest, open space) in various buffer distances
log10_trucking	N/A	N/A	Log_{10} meters to trucking company
log10.caline <type><buffer>	Cars.sm, Cars.wn, Trux.sm, Trux.wn	1500m, 3000m, 4500m	CAL3QHCR car- and truck-source pollution estimates in various buffer distances in summer and winter
<type>LogBuff <buffer>	bc, uv	300m, 500m	Mean of log_{10} mobile monitoring values in black carbon and ultraviolet channels in various buffer distances

Variables were excluded from consideration if they were correlated by greater than 95% with another variable that appeared previously in the dataset. Variables were also excluded if their total change across the study area was less than 10% or if their coefficient of variation was less than 0.1. The least absolute shrinkage and selection operator (lasso) was then used to select from among the remaining 77 variables. Lasso is a method described by Tibshirani (1996) that selects a model to minimize the sum of squared residuals and the absolute value of the model coefficients. The lasso estimate $(\hat{\alpha}, \hat{\beta})$ for a set of standardized x_{ij} is defined by Equation 3:

$$(\hat{\alpha}, \hat{\beta}) = argmin \left\{ \sum_{i=1}^{N} \left(y_1 - \alpha - \sum_{j} \beta_j x_{ij} \right)^2 \right\} subject\ to\ \sum_{j} |\beta_j| \leq t$$

Equation 4. The lasso equation

The constraint on $\sum_j |\beta_j|$ is defined by the value of the lasso penalty t. The optimal value of t to minimize the mean-square error for each model was selected by five-fold cross-validation. Cross-validation groups were randomly selected, with any sites closer than 250 meters kept in the same group.

Reverse stepwise regression was performed on the model terms selected by the lasso method to minimize the Akaike Information Criterion (AIC). Due to the small number of active sampling sites (n=20), the lasso and stepwise procedures were repeated 500 times for each model to ensure their stability as cross-validation groups were randomly rearranged. The performance of the final models was assessed using leave-one-out cross-validation, with the exception of NO_x models, which were assessed using 10 randomly selected cross-validation groups. These statistical analyses were conducted in R version 2.15.2.

Predictions were calculated from land-use regression equations for a grid of points 50 meters apart across the study area for 1-NP, BC and pollution score, and 100 meters apart for NO_x. Universal kriging was applied to these points to generate a smoothed raster surface of the gradient of predictions for each of the seven models using ArcGIS 10.1. Kriging is a minimum mean-squared error technique for interpolating a prediction surface between points with fixed values. The universal kriging tool in ArcGIS assumes spatial correlation based on a linear semivariogram with linear drift (Mercer et al., 2011).

Vehicle counts at the majority of sampling sites were also collected to supplement pollution measurements. The methods and results of the traffic count campaign are described in detail in Appendix-1.

RESULTS

MONITORING RESULTS

The measurement results from the August and December sampling campaigns in the core study area are summarized in Table 4.

Table 4. Summary of measured pollutant levels (core study area)

	Mean	Median	Standard Deviation	Minimum	Maximum
August 18-30					
1-Nitropyrene (pg/m^3)	0.66	0.49	0.51	0.26	2.5
BC (10^{-6} m^{-1})	5.6	5.1	1.1	4.3	7.8
NO_x (ppb)	30.	29	11	19	74
NO_2 (ppb)	14	13	3.6	8.2	26
$PM_{2.5}$ (µg/m^3)	5.7	5.7	0.7	4.7	7.4
December 1-14					
1-Nitropyrene (pg/m^3)	2.1	1.9	0.99	1.1	5.7
BC (10^{-6} m^{-1})	7.5	7.4	8.3	6.3	9.4
NO_x (ppb)	42	37	17	23	110
NO_2 (ppb)	21	20.	7.3	9.0	49
$PM_{2.5}$ (µg/m^3)	5.2	5.1	0.4	4.4	5.9

The matrix in Figure 11 shows Pearson correlation coefficients and scatterplots between log-transformed pollutants and between seasons, with the exception of $PM_{2.5}$

results. $PM_{2.5}$ concentrations in both August and December were not variable enough to merit further statistical analysis or modeling. In each season, $\log_{10}$ 1-NP and BC concentrations were highly correlated ($r > 0.7$) with each other and were moderately correlated ($r > 0.6$) with NO_x concentrations. The correlation coefficients between August and December log-transformed levels of each individual pollutant ranged from 0.68 – 0.83.

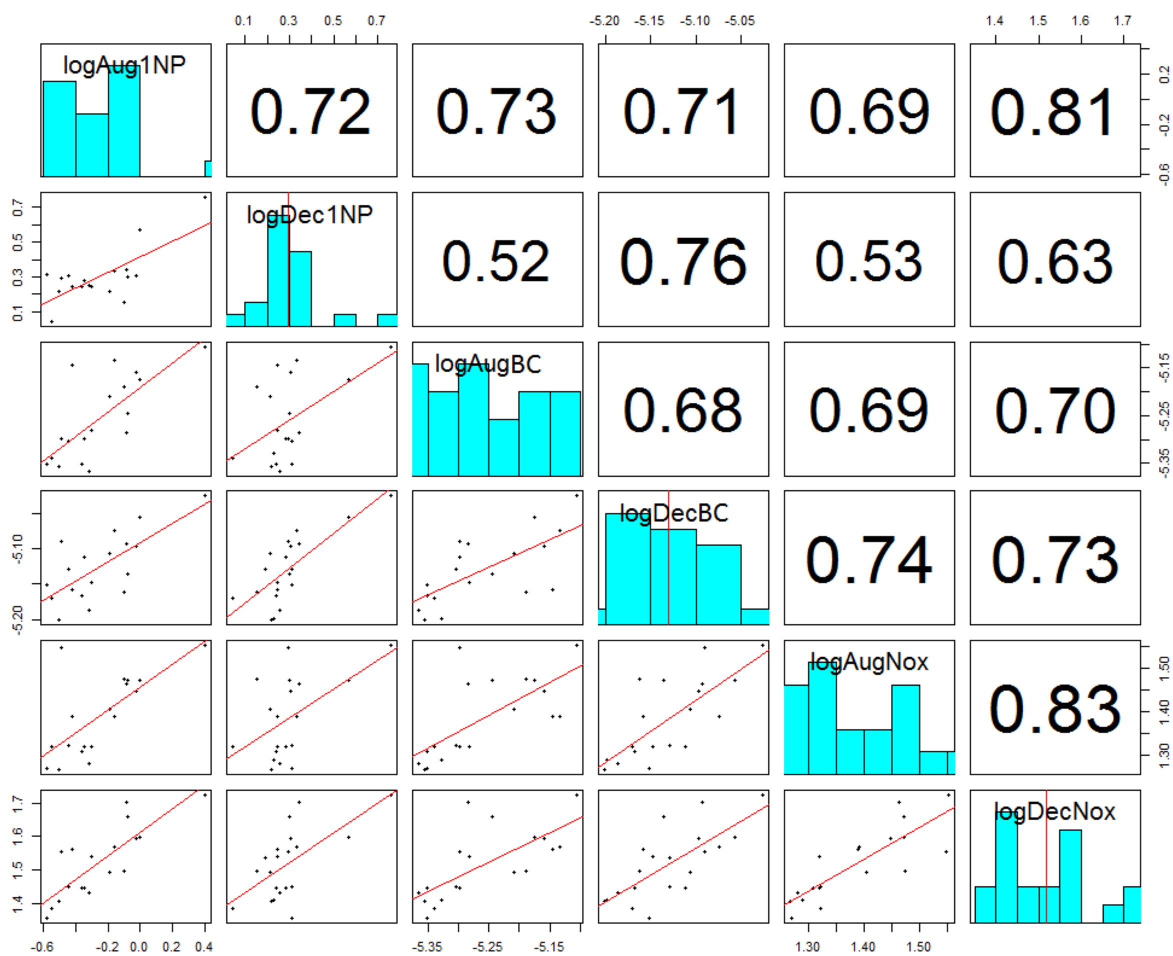

Where *logAug1NP* = Log_{10} August 1-NP measurements
logDec1NP = Log_{10} December 1-NP measurements
logAugBC = Log_{10} August BC measurements
logDecBC = Log_{10} December BC measurements
logAugNox = Log_{10} August NO_x measurements
logDecNox = Log_{10} December NO_x measurements

Figure 11. Correlation matrix of measurement results in August and December

Higher levels of pollutants were observed in December than August, as expected with the differences in meteorological conditions between seasons, with the exception of $PM_{2.5}$. At sites where measurements were available from both seasons, levels of BC were on average 36% higher in December than in August, and NO_x concentrations were 44% higher in December. Concentrations of $PM_{2.5}$ were an average of 12% higher in August than December. While 1-NP concentrations were over 3 times higher in December, photodegradation of 1-NP in summer likely contributed to this larger difference.

Figures 11-18 below display the measured levels of 1-NP, BC and NO_x and the pollution scores in both seasons. Symbol colors were classified using the Jenks natural breaks classification method.

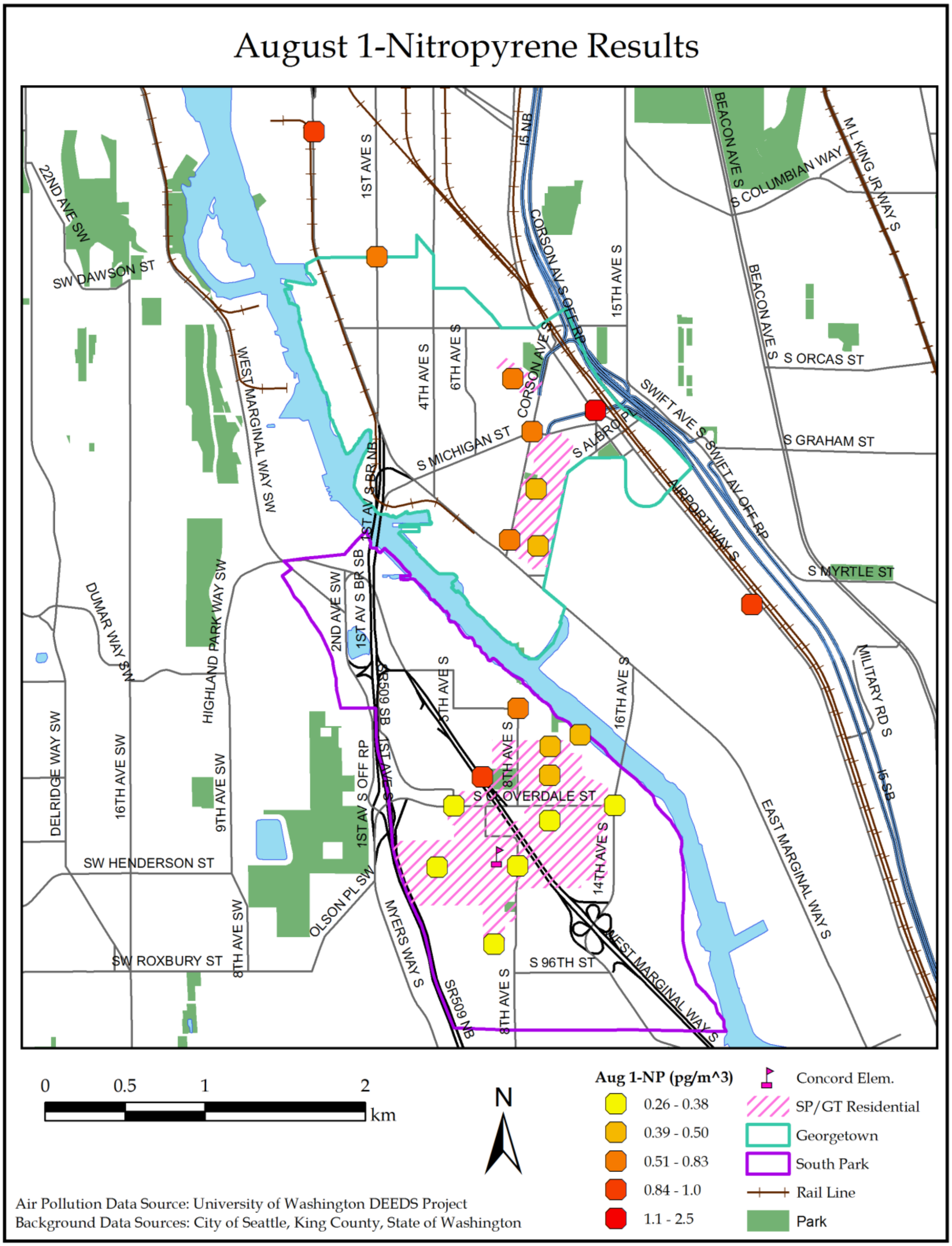

Figure 12. August 1-NP sampling results. Home/business sites were generalized to the nearest intersection.

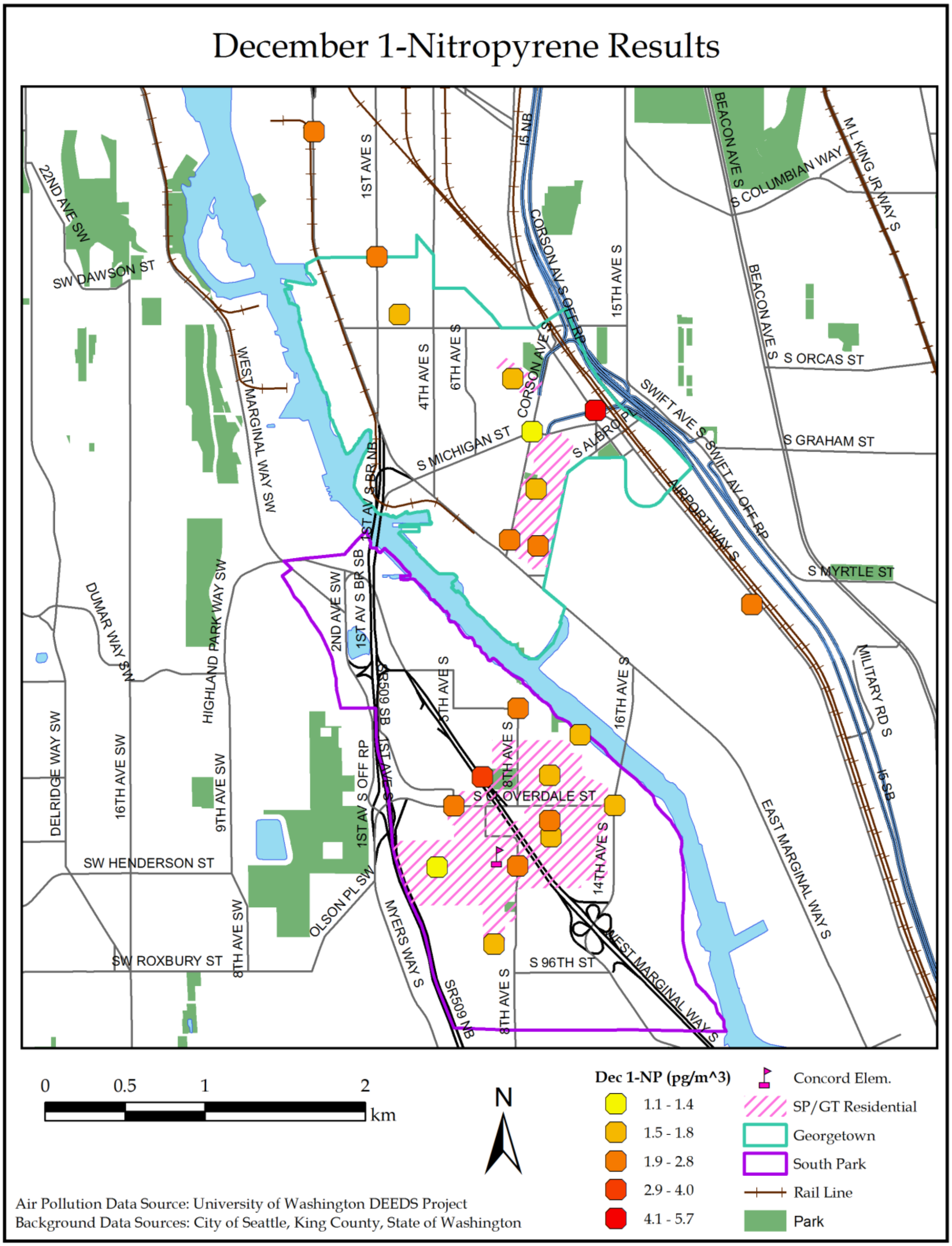

Figure 13. December 1-NP sampling results. Home/business sites were generalized to the nearest intersection.

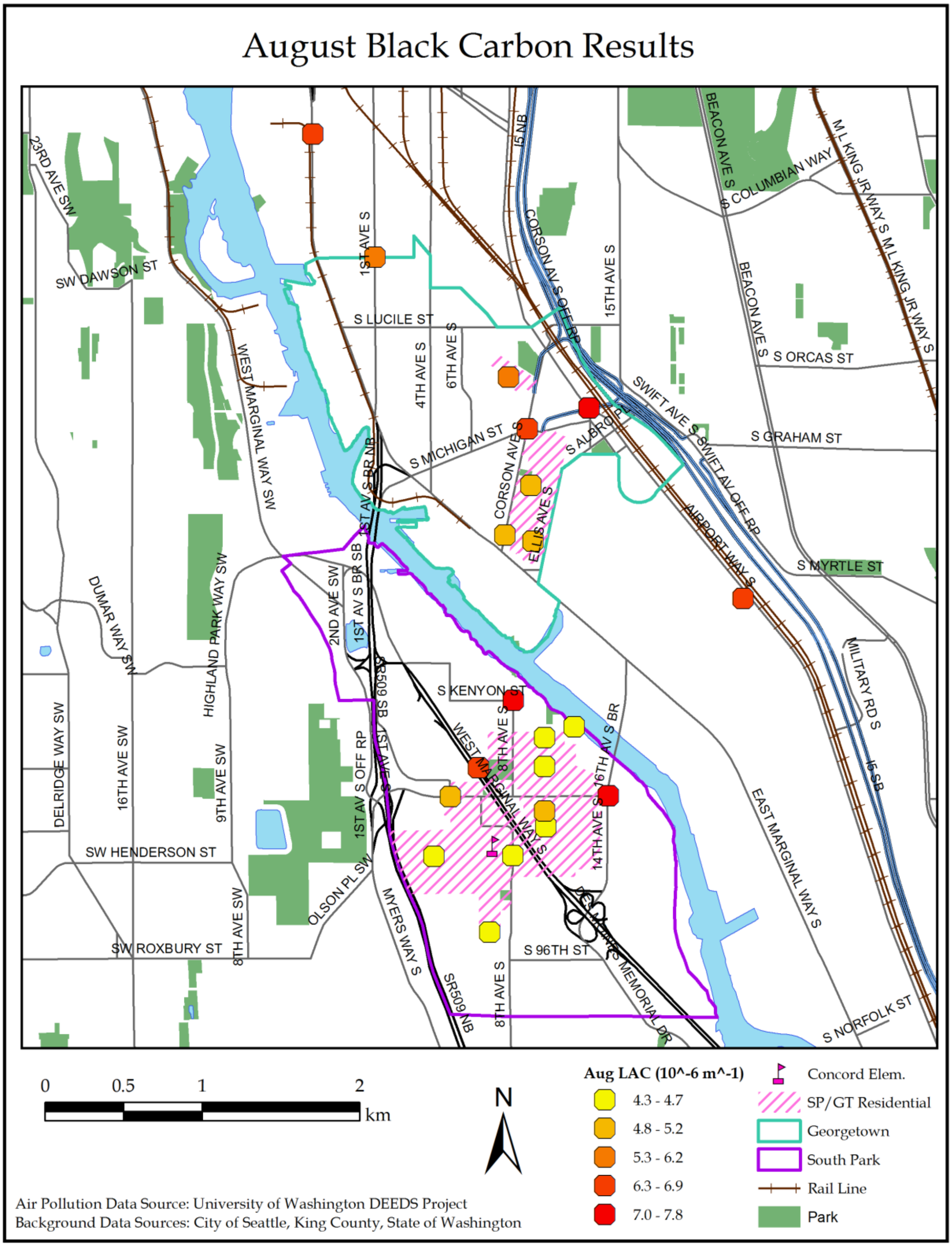

Figure 14. August BC sampling results. Home/business sites were generalized to the nearest intersection.

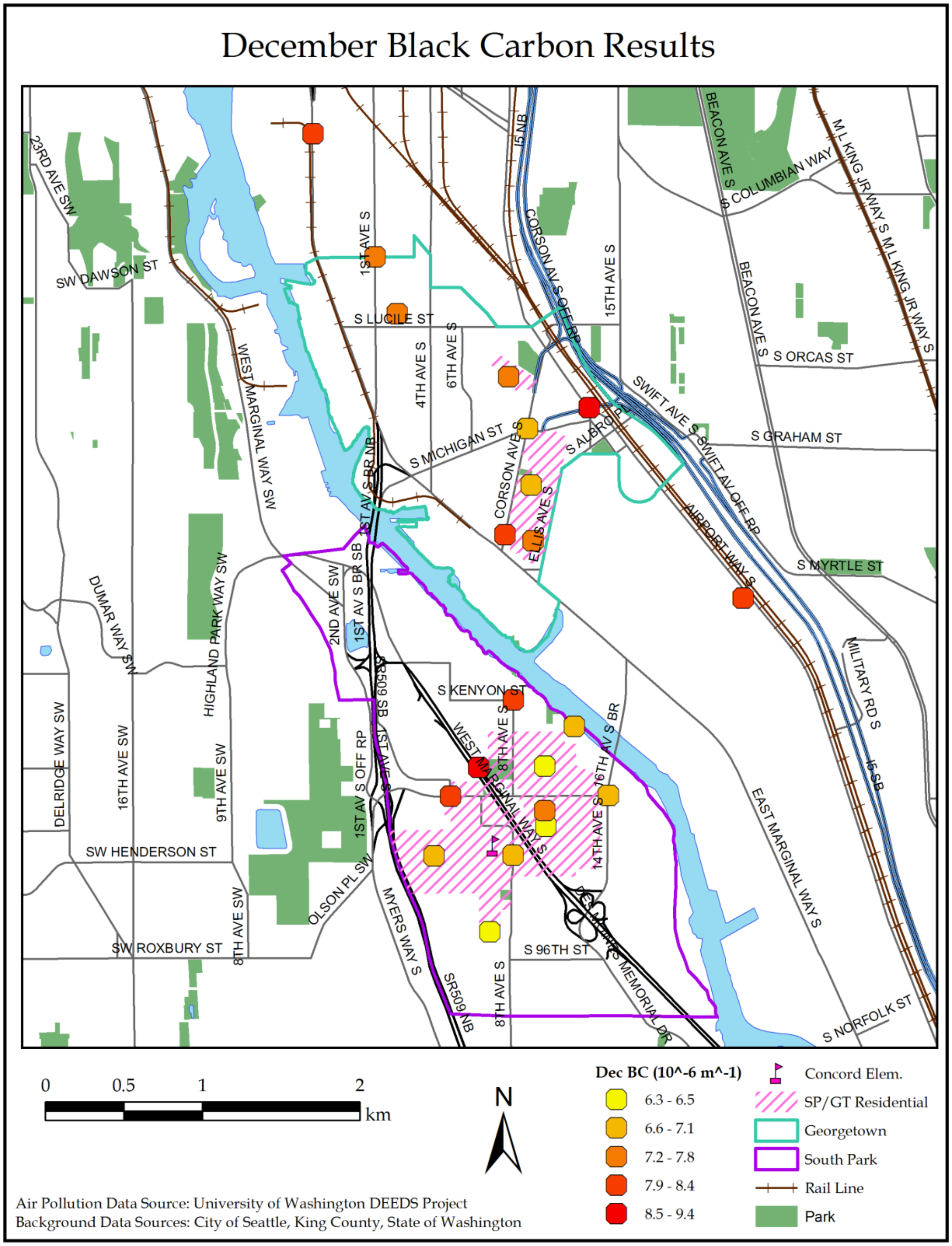

Figure 15. December BC sampling results. Home/business sites were generalized to the nearest intersection.

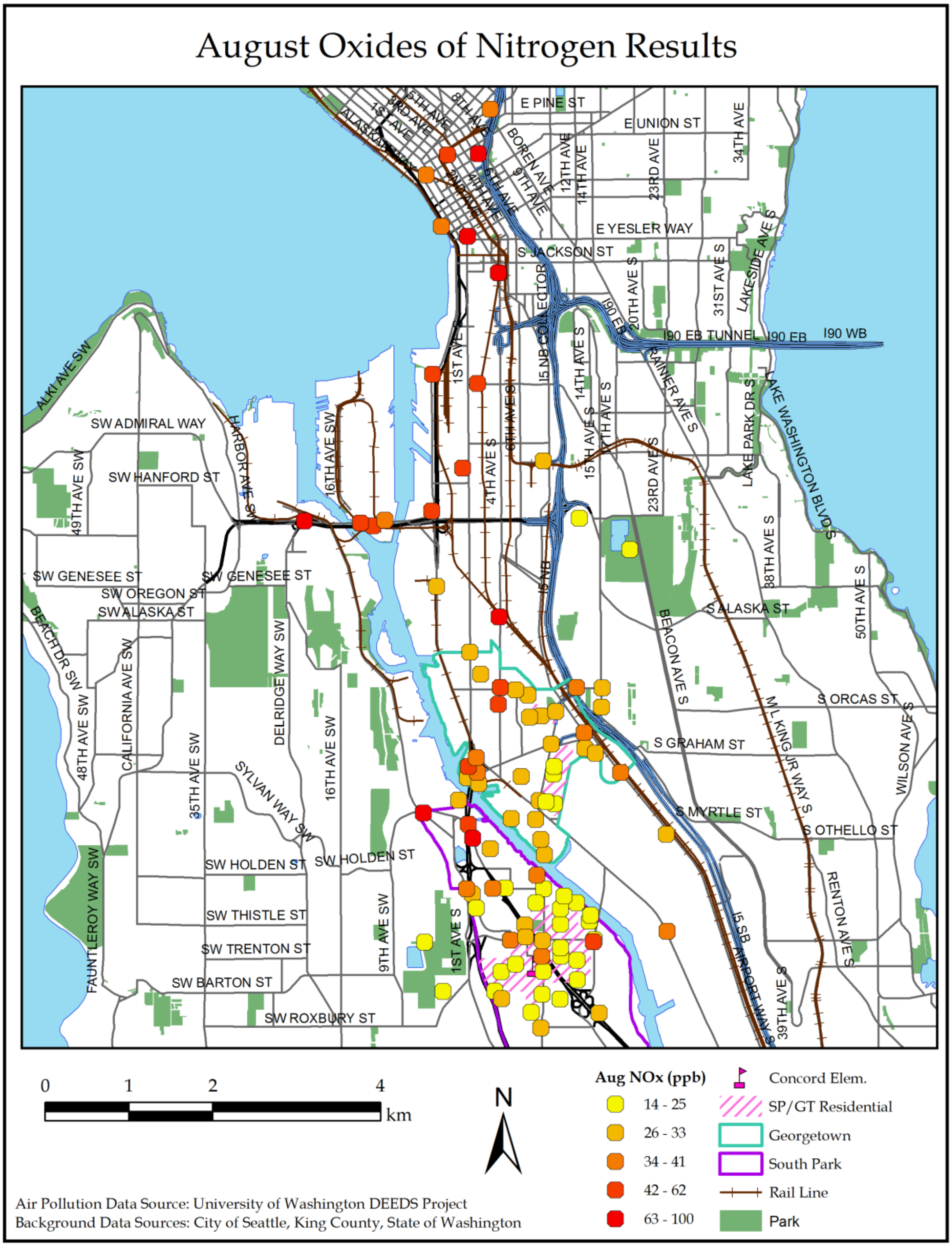

Figure 16. August NO_x sampling results. Home/business sites were generalized to the nearest intersection.

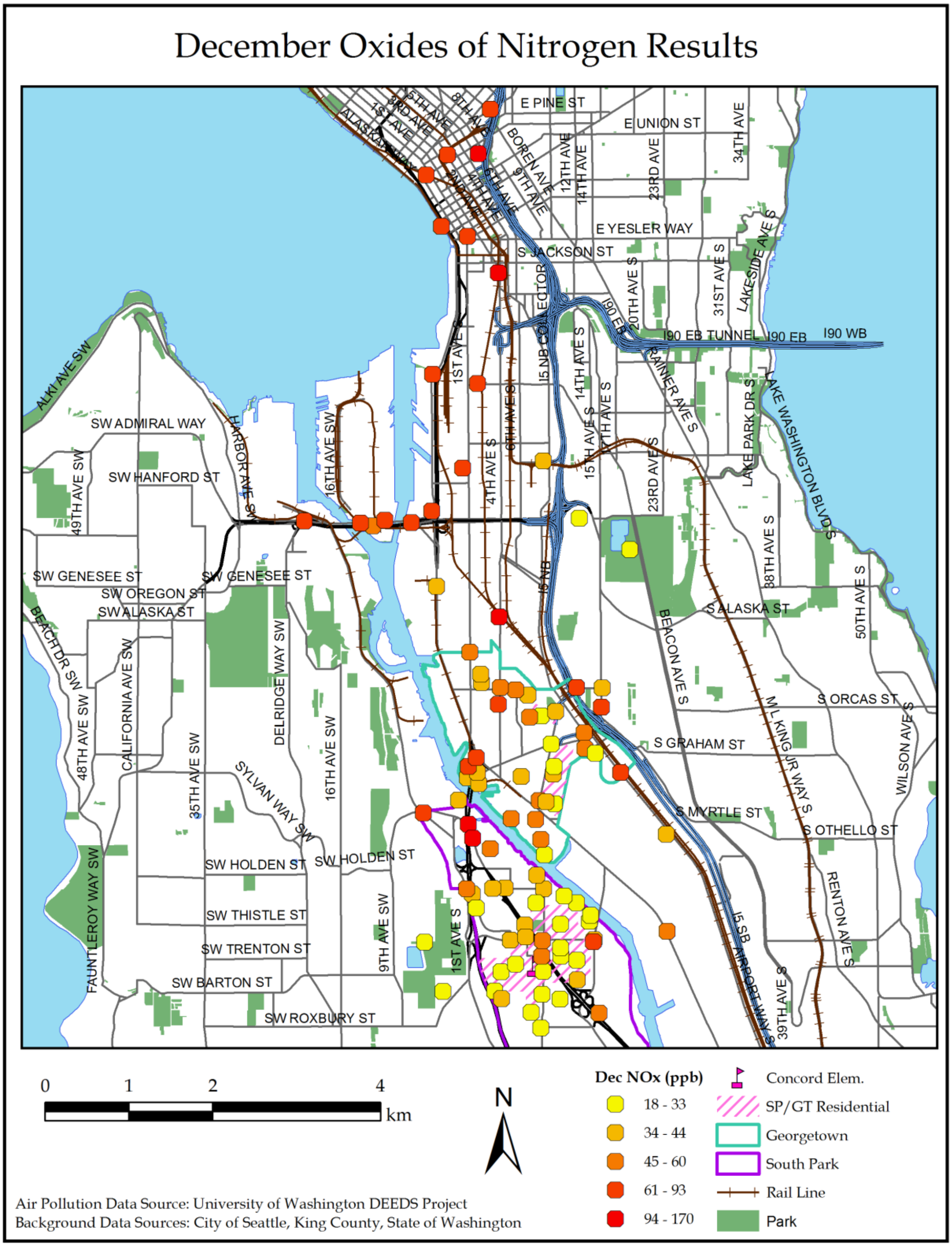

Figure 17. December NOx sampling results. Home/business sites were generalized to the nearest intersection.

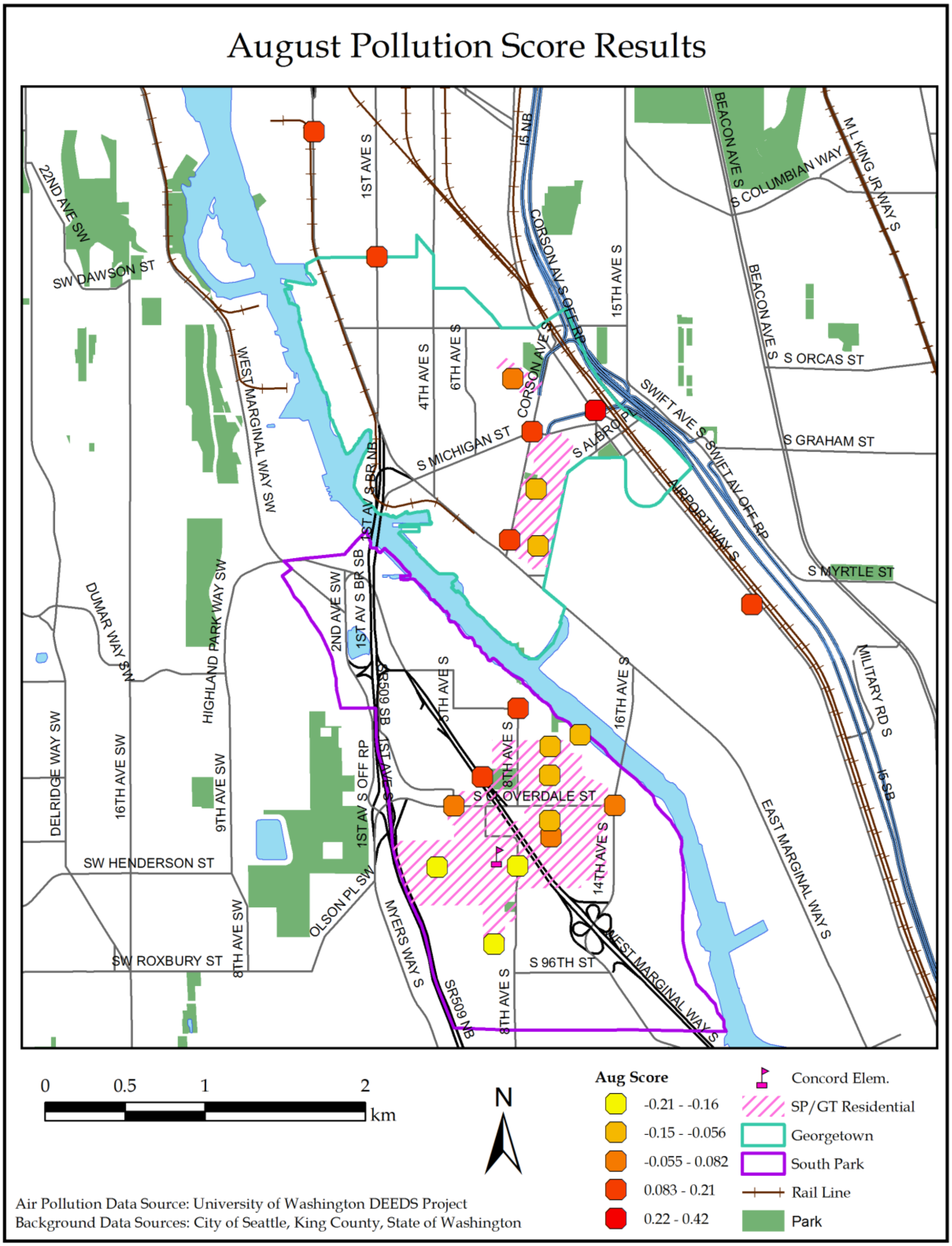

Figure 18. August pollution score results. Home/business sites were generalized to the nearest intersection.

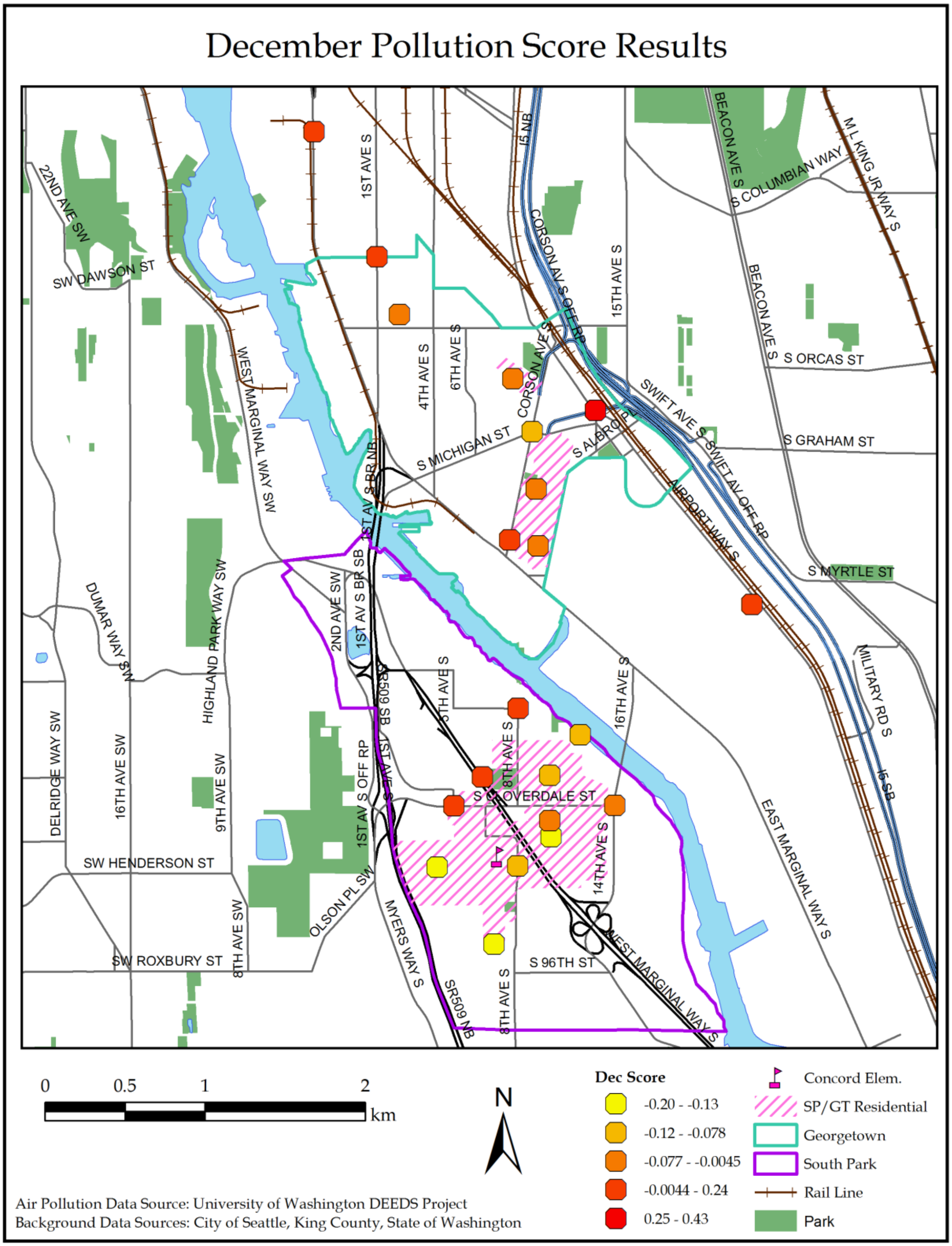

Figure 19. December pollution score results. Home/business sites were generalized to the nearest intersection.

MODELING RESULTS

August 1-Nitropyrene

The spatial covariates included in the model of $\log_{10}$ August 1-NP are summarized in Table 5 below. Figure 20 shows the gradient of August 1-NP predictions across the core study area.

Table 5. $\mathbf{Log_{10}}$ August 1-NP model terms

Variable	Coefficient	Std. Error	t-value	p-value[1]	95% CI
$\mathbf{Log_{10}}$ meters to railroad	-0.18	0.081	-2.2	0.04	(-0.36, -0.0061)
High-intensity development[2] in 150m	0.0025	0.0010	2.4	0.03	(0.00030, 0.0047)
$\mathbf{Log_{10}}$ CAL3QHCR truck emission predictions in 4500m	0.29	0.20	1.5	0.16	(-0.13, 0.71)
Mean $\mathbf{log_{10}}$ mobile black carbon in 300m	1.3	0.41	3.2	0.01	(0.43, 2.2)
Model $\mathbf{R^2}$ = 0.87 **Cross-validated $\mathbf{R^2}$ =** 0.73 **Cross-validated RMSE =** 0.12 $\log_{10}$ pg/m^3					

[1] p-values reflect significance of the association between the variable and the outcome.

[2] "Developed high intensity" areas are defined as "highly developed areas where people reside or work in high numbers. Examples include apartment complexes, row houses and commercial/industrial. Impervious surfaces account for 80% to 100% of the total cover" (MRLC, 2006).

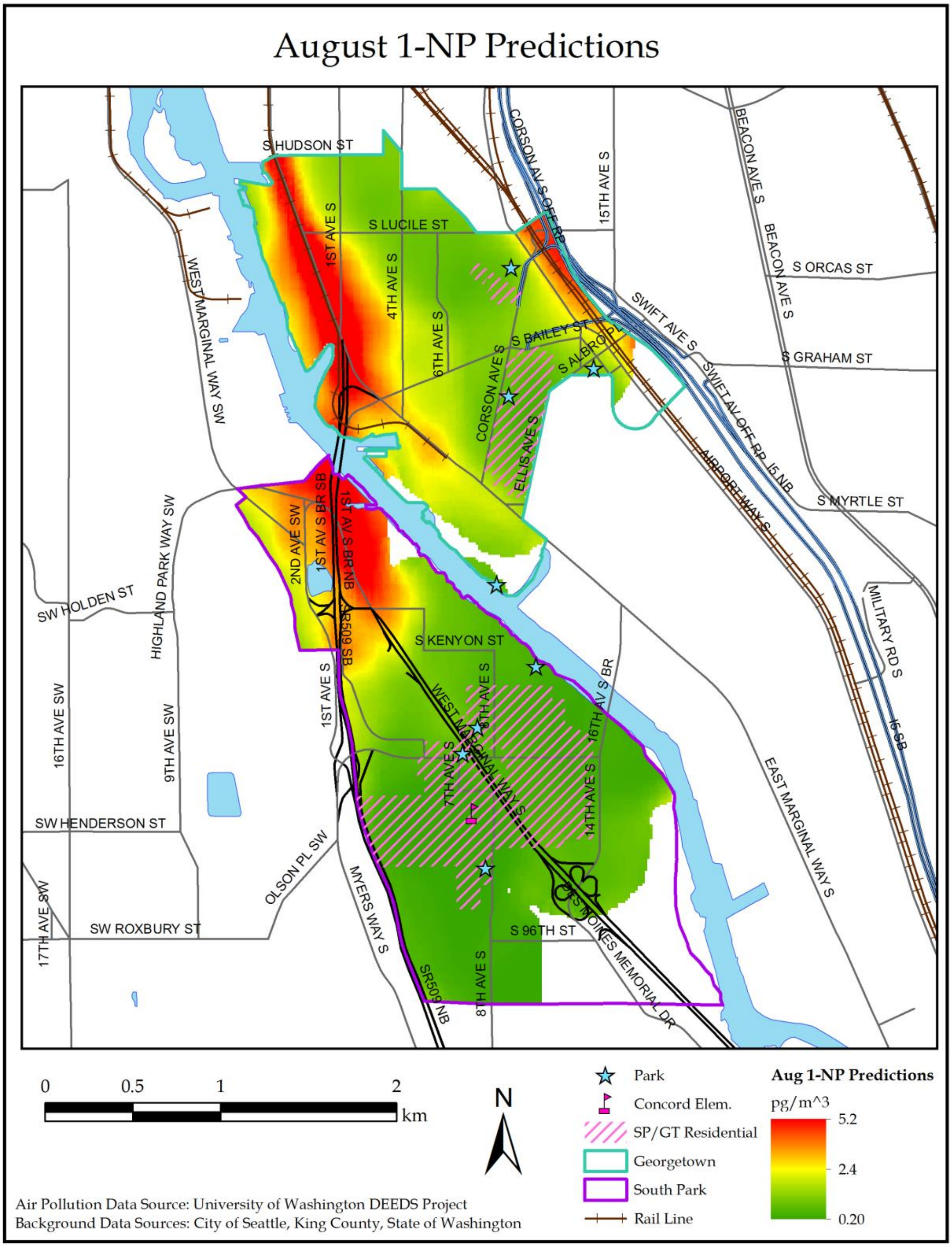

Figure 20. Map of August 1-NP prediction gradient

December 1-Nitropyrene

December 1-NP was found to be unsuitable for spatial modeling because of a low coefficient of variation (0.49) and low signal-to-noise ratio within residential neighborhoods where the majority of sites were located. The lasso procedure consistently yielded a model with 0 variables, indicating that the mean measured concentration in December was a better predictor of winter 1-NP across the neighborhoods than any of the spatial covariates.

August Black Carbon

The spatial covariates included in the model of $\log_{10}$ August BC are summarized in Table 6 below. Figure 21 shows the gradient of August BC predictions across the study area.

Table 6. Log_{10} August BC model terms

Variable	Coefficient	Std. Error	t-value	p-value	95% CI
Log_{10} meters to intersection	-0.067	0.032	-2.1	0.05	(-0.13, 0.0015)
Area of impervious surface in 150m	0.0027	0.00056	4.7	<0.001	(0.0015, 0.0038)
Log_{10} CAL3QHCR truck emission predictions in 4500m	0.17	0.0078	2.2	0.04	(0.0085, 0.34)
Model R^2 = 0.78 **Cross-validated R^2 =** 0.66 **Cross-validated RMSE =** 0.049 $\log_{10}$ m^{-1}					

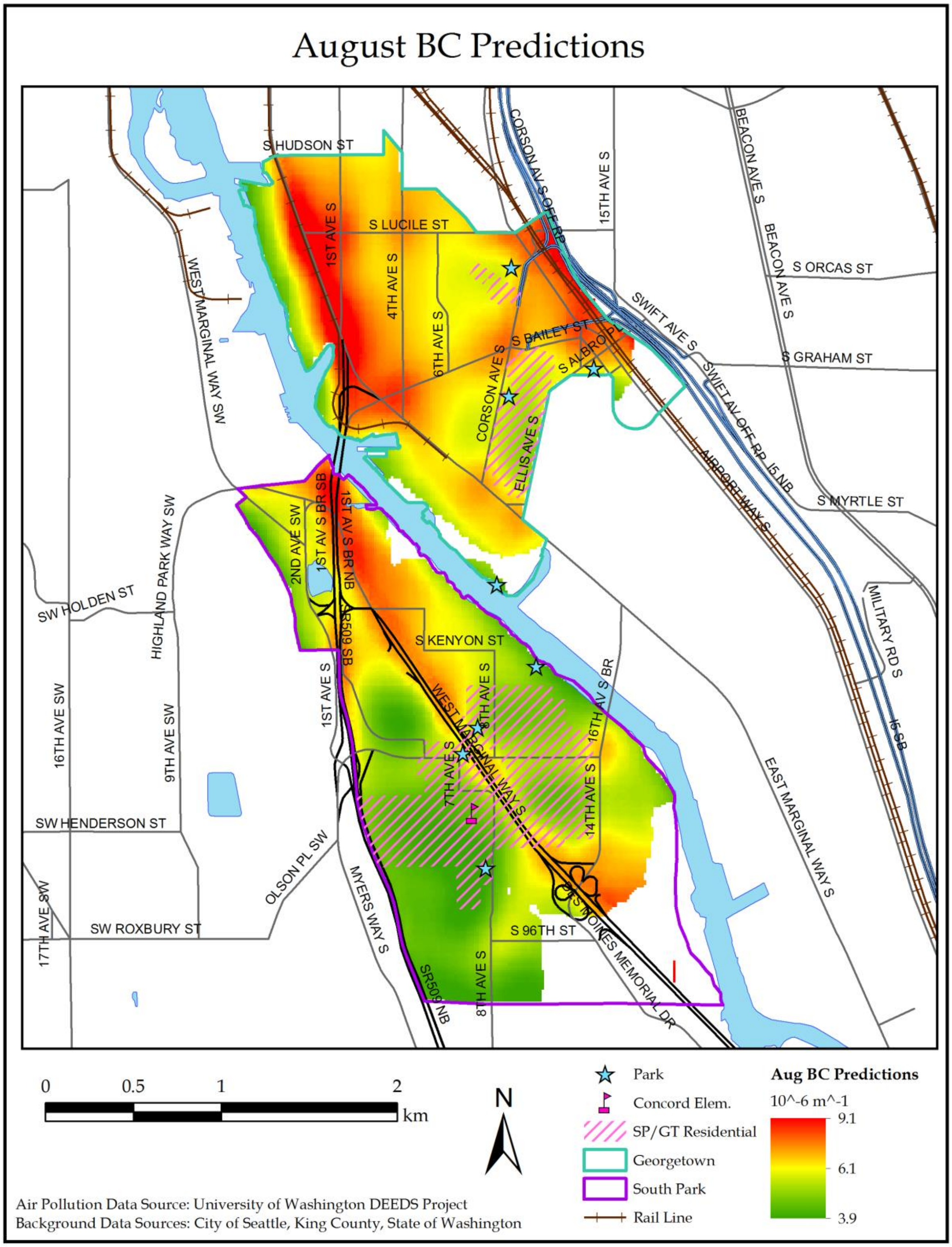

Figure 21. Map of August BC prediction gradient

December Black Carbon

The spatial covariates included in the model of $\log_{10}$ December BC are summarized in Table 7 below. Figure 22 shows the gradient of December BC predictions across the core study area.

Table 7. Log_{10} December BC model terms

Variable	Coefficient	Std. Error	t-value	p-value	95% CI
Log_{10} meters to A1 road[3]	-0.063	0.020	-3.2	0.01	(-0.10, -0.21)
Medium- and high-intensity development[4] **in 150m**	0.0012	0.00025	5.0	<0.001	(0.00072, 0.0018)
Mean $\log_{10}$ mobile black carbon in 300m	0.23	0.11	2.1	0.06	(-0.077, 0.47)
Model R^2 = 0.79 **Cross-validated R^2 =** 0.69 **Cross-validated RMSE =** 0.026 $\log_{10}$ m^{-1}					

[3] A1 roads consist of interstates, state highways and the upper West Seattle bridge.

[4] In addition to the high intensity areas described in the August 1-NP model, the rlc.dev.medhi.p00150 land use category also includes medium intensity development, which is defined as “areas with a mixture of constructed materials and vegetation. Impervious surfaces account for 50% to 79% of the total cover. These areas most commonly include single-family housing units” (MRLC, 2006).

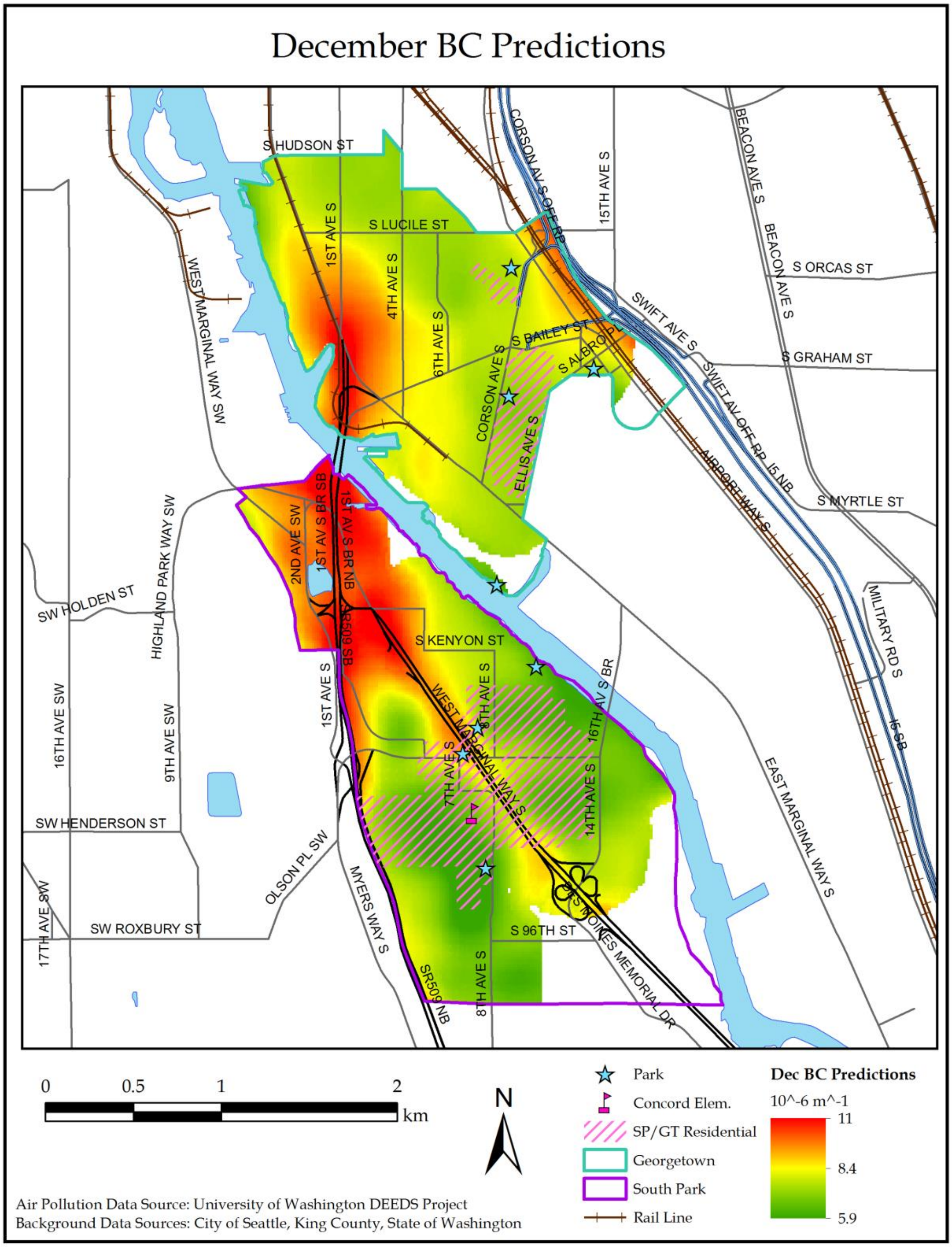

Figure 22. Map of December BC prediction gradient

August NOx

The spatial covariates included in the model of $\log_{10}$ August NO_x are summarized in Table 8 below. Figure 23 shows the gradient of August NO_x predictions. The broader geographic extent of the NO_x prediction surface on these maps reflects the wider distribution of NO_x sampling sites.

Table 8. Log10 August NO_x model terms

Variable	Coefficient	Std. Error	t-value	p-value	95% CI
$\log_{10}$ meters to the Port of Seattle	-0.10	0.038	-2.7	0.0078	(-0.18, -0.028)
$\log_{10}$ meters to road	-0.069	0.034	-2.0	0.044	(-0.14, -0.0019)
Length of A2 and A3 roads in 100m	0.00017	0.00011	1.6	0.12	(-0.000046, 0.00039)
High-intensity development in 150m	0.00093	0.00043	2.2	0.032	(0.000081, 0.0018)
High-intensity development in 750m	0.0015	0.00061	2.5	0.013	(0.00033, 0.0028)
$\log_{10}$ CAL3QHCR car emission predictions in 4500m	0.21	0.056	3.7	<0.001	(0.095, 0.32)
Model R^2 = 0.74 **Cross-validated R^2 =** 0.68 **Cross-validated RMSE =** 0.097 $\log_{10}$ ppb					

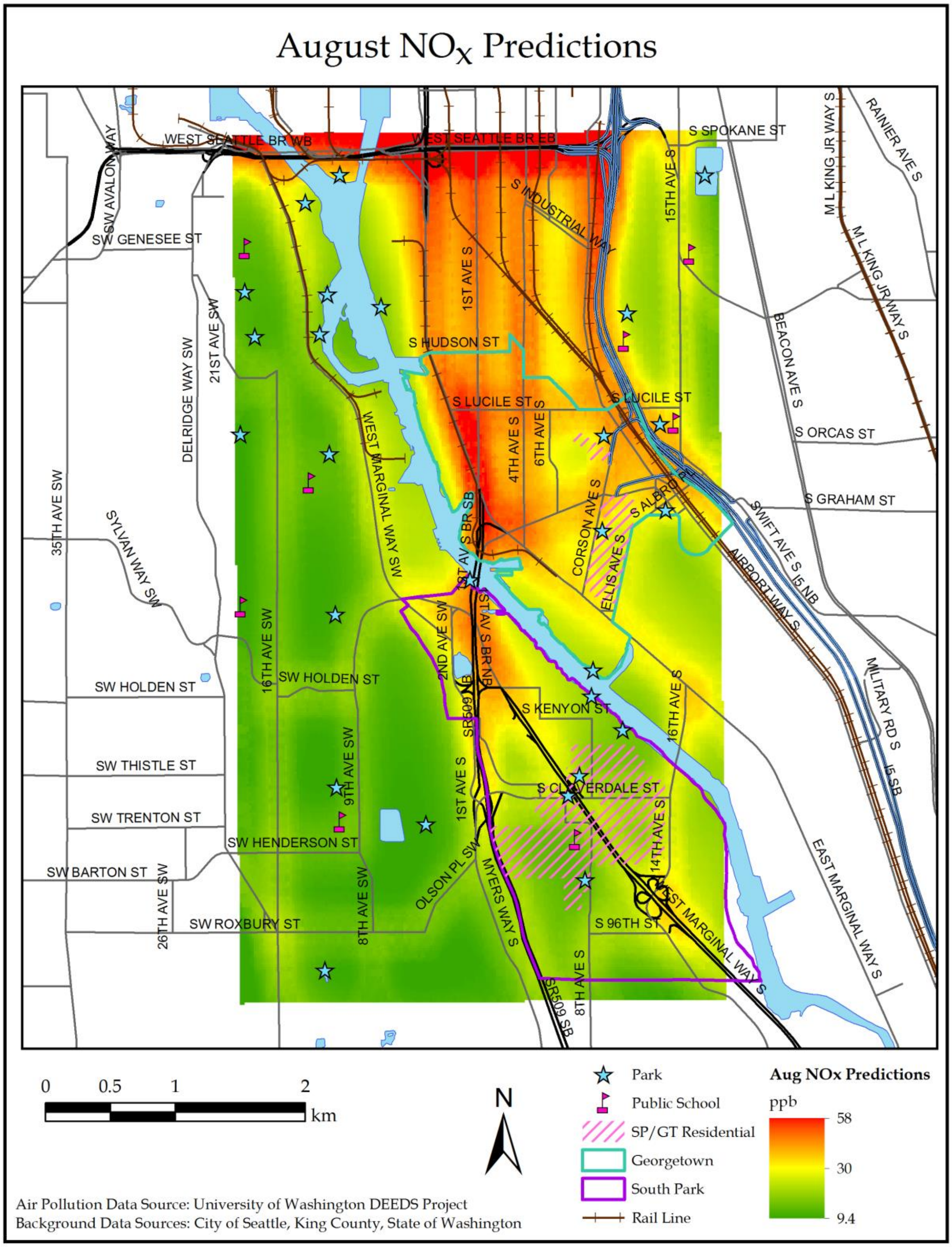

Figure 23. Map of August NO_x prediction gradient

December NOx

The spatial covariates included in the model of $\log_{10}$ December NO_x are summarized in Table 9 below. Figure 24 shows the gradient of December NO_x predictions.

Table 9. Log_{10} December NO_x model terms

Variable	Coefficient	Std. Error	t-value	p-value	95% CI
Log_{10} meters to railroad	-0.099	0.028	-3.6	0.001	(-0.15, -0.044)
Log_{10} meters to road	-0.12	0.026	-4.8	<0.001	(-0.18, -0.073)
Length of A1 roads in 1500m	0.000018	0.0000045	3.9	<0.001	(0.0000086, 0.000027)
High-intensity development in 750m	0.0023	0.00049	4.7	<0.001	(0.0013, 0.0033)
Log_{10} CAL3QHCR car emission predictions in 4500m	0.25	0.056	4.5	<0.001	(0.14, 0.36)
Model R^2 = 0.75 **Cross-validated R^2 =** 0.70 **Cross-validated RMSE =** 0.10 $\log_{10}$ ppb					

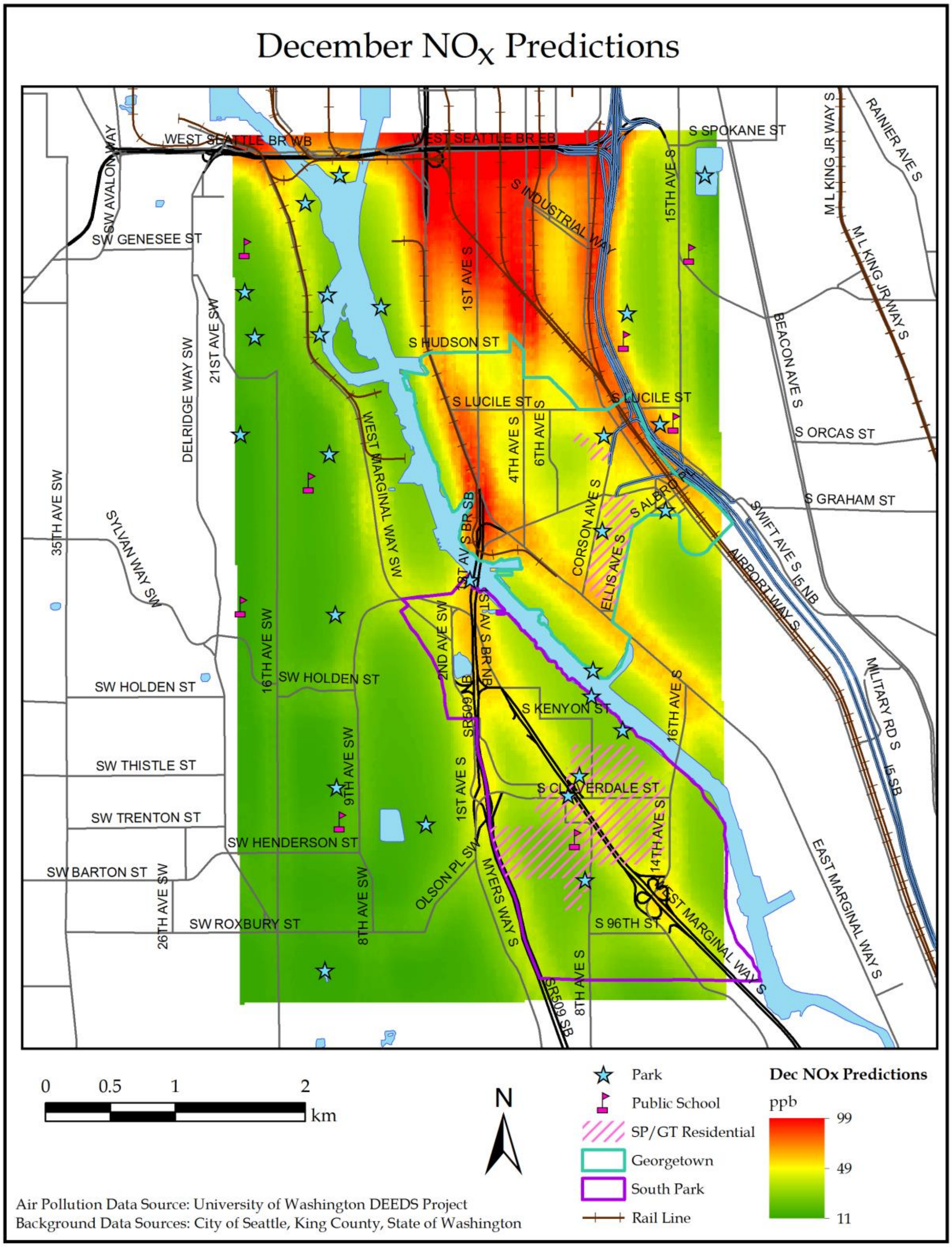

Figure 24. Map of December NO_x prediction gradient

August Pollution Score

The spatial covariates included in the model of August pollution score are summarized in Table 10 below. Figure 25 shows the gradient of August pollution score predictions across the study area.

Table 10. August pollution score model terms

Variable	Coefficient	Std. Error	t-value	p-value	95% CI
Log_{10} meters to intersection	-0.067	0.033	-2.0	0.06	(-0.14, 0.0030)
High-intensity development in 150m	0.0029	0.00038	7.6	<0.001	(0.0021, 0.0037)
Log_{10} CAL3QHCR truck emission predictions in 4500m	0.30	0.083	3.6	0.002	(0.12, 0.48)
Mean log_{10} mobile black carbon in 300m	0.79	0.18	4.3	0.001	(0.40, 1.2)
Model R^2 = 0.94 **Cross-validated R^2 =** 0.89 **Cross-validated RMSE =** 0.054					

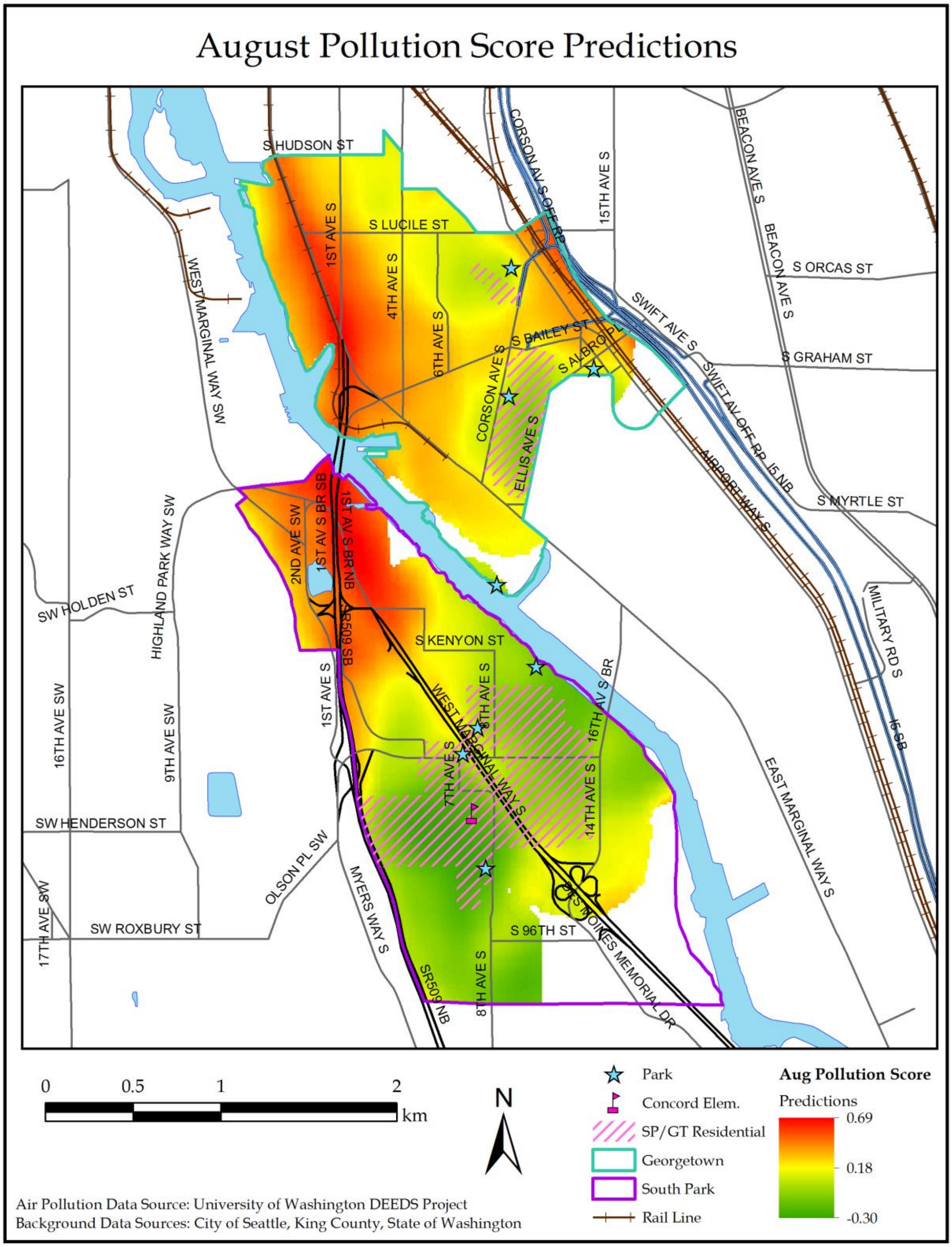

Figure 25. Map of August pollution score predictions

December Pollution Score

The spatial covariates included in the model of December pollution score are summarized in Table 11 below. Figure 26 shows the gradient of December pollution score predictions across the study area.

Table 11. December pollution score model terms

Variable	Coefficient	Std. Error	t-value	p-value	95% CI
Area of impervious surface in 50m	0.0029	0.00091	3.2	0.005	(0.00098, 0.0048)
Mean $\log_{10}$ mobile black carbon in 300m	1.2	0.31	3.8	0.001	(0.52, 1.8)
Model R^2 = 0.70 **Cross-validated R^2 =** 0.58 **Cross-validated RMSE =** 0.092					

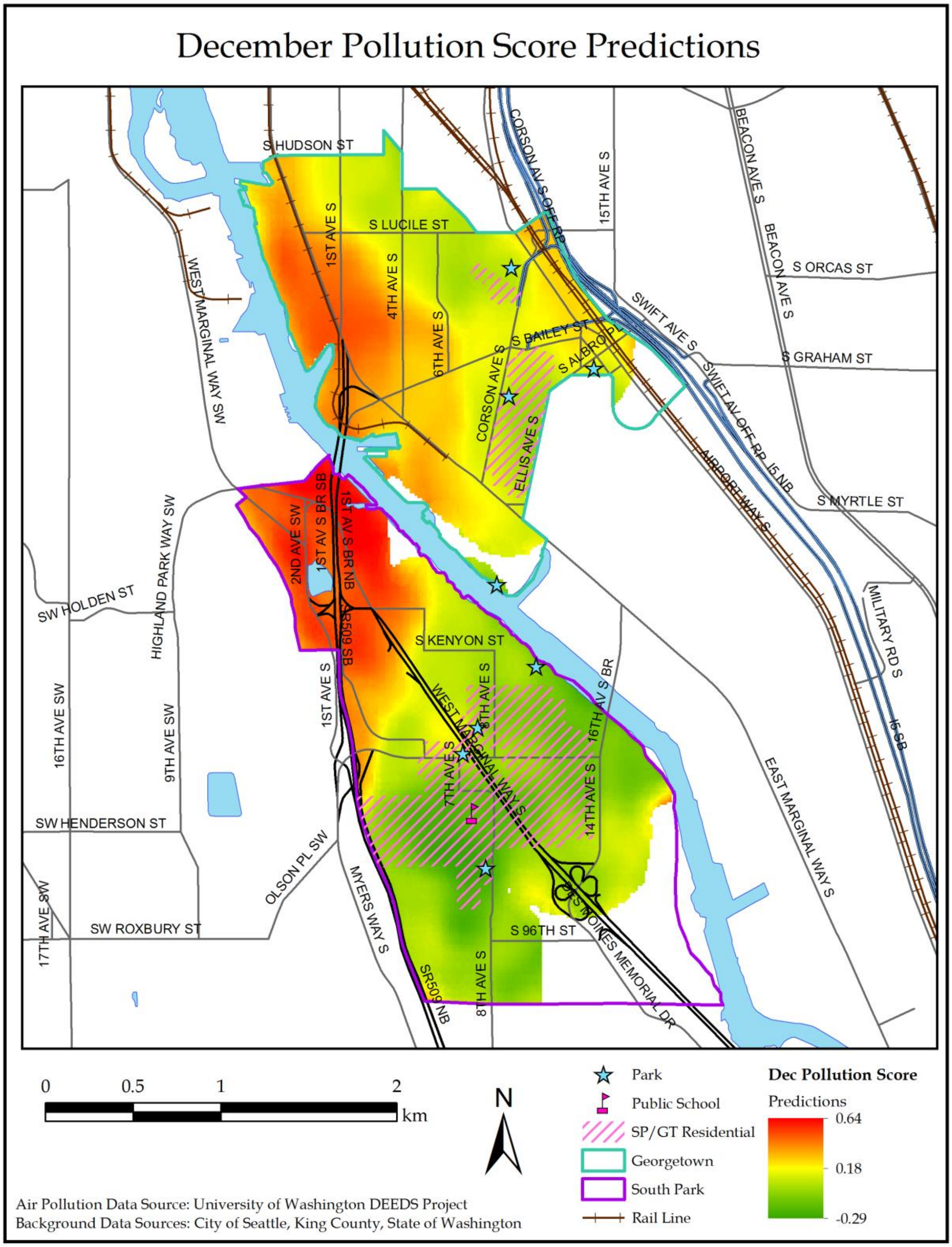

Figure 26. Map of December pollution score predictions

For correlation matrices of covariates in the above models, see Appendix-7. For maps of model residuals, see Appendix-14.

MODEL PERFORMANCE

The performance statistics for each model are reported again in Table 12 below for ease of comparison. Statistics are reported both in the log_{10} units used to develop the models and in the original units, where exponentiated predictions are compared to the original measurements. For scatterplots of cross-validated model predictions and measured values, see Appendix-21.

Table 12. Summary of model performance statistics

Model	Model R^2	Cross-Validated R^2 (Log_{10} Units)	Cross-validated RMSE (Log_{10} Units)	Cross-validated R^2 (Original Units)	Cross-validated RMSE (Original Units)
August 1-NP	0.87	0.73	0.12 log_{10} pg/ m^3	0.64	0.30 pg/m^3
August BC	0.78	0.66	0.049 log_{10} m^{-1}	0.65	6.6 x 10^{-6} m^{-1}
December BC	0.79	0.69	0.026 log_{10} m^{-1}	0.70	4.5 x 10^{-6} m^{-1}
August NO_x	0.74	0.68	0.097 log_{10} ppb	0.54	11 ppb
December NO_x	0.75	0.70	0.10 log_{10} ppb	0.61	15 ppb
August Pollution Score	0.94	N/A	N/A	0.89	0.054
December Pollution Score	0.70	N/A	N/A	0.58	0.092

SUMMARY OF PREDICTED VALUES

The mean predictions of the three pollutants are summarized in Table 9 by neighborhood, within both the full neighborhood boundaries and areas of residential zoning by neighborhood. The measurement results from the Queen Anne and Beacon Hill agency sites are included for comparison.

Table 13. Mean predictions by neighborhood with comparison site measurements

	Georgetown Mean*	South Park Mean*	Georgetown Residential Mean*	South Park Residential Mean*	Queen Anne Agency Site**	Beacon Hill Agency Site**	Down-town Agency Site**
August 1-NP (pg/m^3)	1.6	0.91	0.63	0.38	0.21	0.34	1.0
August BC (10^{-6} m^{-1})	6.5	5.5	5.7	5.0	1.7	4.2	6.8
December BC (10^{-6} m^{-1})	8.2	8.0	7.4	7.2	4.2	4.2	9.6
August NO_x (ppb)	34	26	29	22	14	18	37
December NO_x (ppb)	47	35	43	33	24	21	71
August pollution score	0.27	0.099	0.026	-0.097	-0.57	-0.21	0.28
December pollution score	0.21	0.098	0.049	-0.095	-0.42	-0.46	0.43

* Mean of predictions
**Measured value

The greatest difference between mean predictions in South Park and Georgetown and measured values at comparison neighborhood sites was observed from the August 1-NP model. As the magnitude of this difference was a key finding from the DEEDS study, the results of the August 1-NP comparison from Table 13 are displayed visually in Figure 27 below.

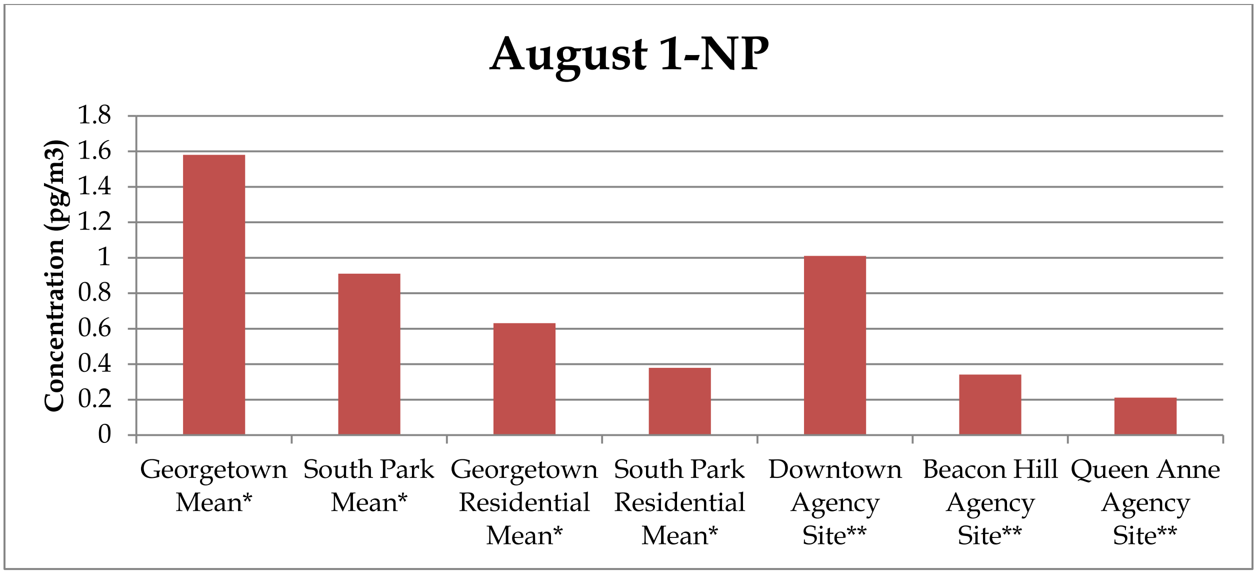

* Mean of predictions
** Measured value

Figure 27. Mean August 1-NP predictions by neighborhood with comparison site measurements

DISCUSSION

Key Findings

This study successfully characterized the gradient of several diesel exhaust markers in two small neighborhoods. This effort not only demonstrates new applications of land-use regression modeling but also provides community members with a better understanding of residential-level exposure to diesel pollutants in South Park and Georgetown. Using direct measurements from a high-density sampling campaign, this study developed finely-resolved models of several pollutants and identified spatial gradations in pollution levels. The modeling results fulfilled the twin aims of identifying key neighborhood features that predict pollution levels and generating gradient maps of pollutants.

Several key findings from the modeling and mapping effort provide insight into the major pollution sources and neighborhood locations of concern. Spatial features that predicted pollution levels varied between pollutants and between seasons, but in general they included road and railroad proximity, industrial activity, and truck emissions. These models indicate that residents near busy roads and industrial areas face the greatest air quality impacts from proximate diesel sources.

A few neighborhood locations consistently saw the highest predicted concentrations from multiple models. These included the 1st Avenue Bridge between South Park and Georgetown, the Georgetown commercial district near Interstate 5, and the Georgetown industrial zone along E Marginal Way S. Several multi-family apartment complexes are located in the Georgetown commercial district, and these models suggest that residents of these buildings may face particularly high levels of diesel pollution. Models of BC and NO_x also show the air quality impacts of state highways, including SR99 that bisects the South Park residential neighborhood. The broader scope of the NO_x gradient maps shows additional areas around SoDo and Harbor Island with some of the area's highest concentrations of NO_x, both measured and predicted.

Measurement results from residential comparison sites suggest that residents of South Park and Georgetown generally face higher levels of pollution than residents of other neighborhoods where sampling took place. Mean predicted levels of all pollutants in the South Park and Georgetown neighborhoods were higher than measured levels at the Queen Anne and Beacon Hill comparison sites, both of which are located atop hills in areas with less commercial truck traffic. Mean predicted levels of all pollutants were higher in Georgetown than in South Park, both in residential zones and in the neighborhoods as a whole.

Concentrations of criteria pollutants measured fell within the U.S. EPA's National Ambient Air Quality Standards (NAAQS). All $PM_{2.5}$ concentrations measured were below both the annual and 24-hour standards for $PM_{2.5}$ (15 $\mu g/m^3$ and 35 $\mu g/m^3$, respectively). All NO_2 concentrations measured were also below both the annual and 1-hour standards for NO_2 (53 ppb and 100 ppb, respectively). However, the sampling protocol (e.g. sampling duration, collection method, and number of samples collected) was not designed to identify compliance with the NAAQS. The NAAQS do not include standards for the diesel-specific markers measured in this study (1-NP and BC), limiting comparability of diesel exhaust to other metropolitan areas.

Mobile Monitoring Considerations

The model selection methods were optimized to achieve the tandem goals of identifying useful pollution models and generating prediction maps. While largely complementary aims, a few tradeoffs did arise between maximizing the accuracy of prediction maps and ensuring that models were informative about underlying sources of pollution. One example of this challenge surfaced when identifying the best use for the thousands of mobile data points collected in the study area. The mobile monitoring route was designed to include multiple loops around sampling sites. Increasing the number of data points near these sampling sites yielded log-mean values that more accurately reflected the intensity of on-road soot emissions at these points. These variables provided rich information about carbon emissions and their impact on measured pollution levels at nearby sampling sites.

Because of the increased mobile data coverage near sampling sites, the availability of data points in other parts of the study area was more limited. To generate prediction maps, log-mean mobile data values were calculated in a 300 meter buffer around each point in the neighborhood grid. The number of data points within 300 meters varied by location, as mobile data coverage was sparser in some areas. These log-mean values were in large part a function of which roads within a 300 meter radius were selected for mobile monitoring in outlying areas. In some cases, the roads selected in this radius were representative of typical roads near these points. In other cases, the mobile route over-sampled smaller roads in a 300 meter radius when larger roads were not covered. In other cases still, the mobile route over-sampled larger roads that were not representative of all roads in a 300 meter area. Consequently, the prediction maps likely over-estimated pollution levels in some outlying areas and under-estimated in others. For the most accurate prediction maps, a more suitable mobile route would cover a representative sample of neighborhood roads evenly distributed throughout the neighborhoods.

Estimates of mobile-source pollution from the CAL3QHCR model were included to complement the mobile data variables, as these estimates have different strengths and limitations. The accuracy of CAL3QHCR pollution predictions is limited because they were based on modeled traffic counts rather than empirical traffic counts. In addition, these traffic counts were estimates of annual average daily traffic and were not specific to the sampling periods. They also were based on traffic patterns modeled before the closure of the 16th Avenue S bridge, which likely introduced an additional gap between the traffic model and the actual traffic patterns during the sampling periods. Though modeled pollution predictions are not as accurate as the measured emissions from the mobile data, the CAL3QHCR model included modeled traffic counts from all arterial roads in the study area. Therefore, it is reasonable to expect that predictions in outlying areas are as accurate as those near sampling sites. The CAL3QHCR variables likely increased the accuracy of the prediction maps in models where they appeared alongside mobile data variables.

Study Timing

As with any short-term or "snapshot" sampling campaign, results from limited time periods were used to make inferences about general seasonal air quality conditions in South Park and Georgetown. The August sampling campaign was conducted during a fairly typical summer period of stagnant and sunny weather. While the sampling period was drier (0.0 inches of total precipitation) than the summer 2012 average (0.022 inches per day), the average wind speed of 4.0 mph was the same during the sampling period and summer 2012 as a whole. Aethalometer® measurements of black carbon concentrations collected by the Puget Sound Clean Air Agency at the SoDo monitoring site averaged 0.92 $\mu g/m^3$ during the sampling period, relatively close to the summer 2012 average of 1.1 $\mu g/m^3$. The December sampling campaign took place during a particularly windy and rainy period, though these conditions were not out of the ordinary for Seattle winter. The average precipitation was higher during the sampling campaign (0.25 inches per day) than all of winter 2012-2013 (0.11 inches per day). The average wind speed was also higher during the sampling campaign (7.0 mph) than during the whole winter season (5.0 mph). Average black carbon concentrations at the SoDo site were lower during the December sampling campaign (1.0 $\mu g/m^3$) than winter as a whole (1.4 $\mu g/m^3$). While both sampling campaigns took place during weather patterns that were relatively typical for the season, results from the December sampling campaign may underestimate winter averages due to the heavier wind and rain.

Another feature of the sampling time frame was that the study was conducted while the 16th Ave. S bridge connecting Georgetown and South Park was closed for reconstruction. The traffic patterns seen during the study period differed from typical traffic patterns during normal bridge operation, and air pollution patterns will likely change once the bridge reopens. Before the bridge closure, King County estimated that the bridge carried approximately 20,000 vehicle trips on an average weekday, roughly 2,800 of which were made by commercial trucks. A traffic impacts analysis estimated that when the bridge closed, the majority of this traffic was diverted to the 1st Avenue S bridge and a smaller portion was diverted to the International Blvd S bridge south of the study area (King County, 2010). If traffic returns to its pre-closure pattern once the bridge reopens, levels of diesel exhaust markers can be expected to fall near the 1st Avenue S bridge and to rise near the 16th Avenue bridge in both South Park and Georgetown. The predictions generated by the DEEDS study may prove useful as estimates of baseline pollution levels near the 16th Avenue bridge in the absence of bridge traffic. Once the bridge reopens, future air quality studies in South Park and Georgetown may be able to estimate the impact of bridge traffic on air quality using comparisons from DEEDS.

Site Selection

The distribution of active sampling sites in this study was notable for its high density (approximately 7 per square mile), though the total number of sites (n=20) was relatively low for land-use regression modeling. Additional NO_x results from a much larger number of sites (n=99) were collected to supplement the information gathered at active sites. Consequently, NO_x models were more stable than models of the other pollutants and prediction was possible over a larger geographic area. Though the scope of the other pollutant predictions was more limited, the sample size was large enough to yield robust models within South Park and Georgetown for each pollutant except winter 1-NP.

The active sampling site distribution was somewhat limited by the availability of suitable sampling locations outside of residential areas in South Park and Georgetown. Active sampling was conducted at 4-5 industrial sites in these neighborhoods, yielding a lower site density in industrial areas than residential areas. To ensure diverse land use representation in sampling locations, NO_x samplers were concentrated more heavily in the industrial areas without active sampling sites. Active sampling was not possible at the Port of Seattle. However, several NO_x samplers were located proximate to port terminals on Harbor Island, and NO_x models showed the highest pollution predictions in the vicinity of these areas. An additional active sampling site at or near the Port of Seattle would likely have captured comparably high levels of 1-NP and BC and enhanced the precision of the upper range of predictions.

December 1-NP

No prediction model was identified for December 1-NP. The most plausible explanation for this is the difference in meteorological conditions between the August and December sampling periods. The August sampling period was relatively stagnant and dry, with an average wind speed of 4.0 mph and 0.0 inches of precipitation. In these stagnant conditions, measured concentrations would be driven largely by local sources, which were well represented by the spatial covariates considered for modeling. The average wind speed during December sampling was slightly higher at 7.0 mph (see Figure 28), and 3.2 inches of precipitation fell during the sampling period. Higher winds and precipitation would likely dilute the effects of local sources, causing greater regional mixing of pollutants and lower overall variability. The absence of an informative December 1-NP model may be explained by the confluence of weather conditions, limited 1-NP sampling experience and field noise.

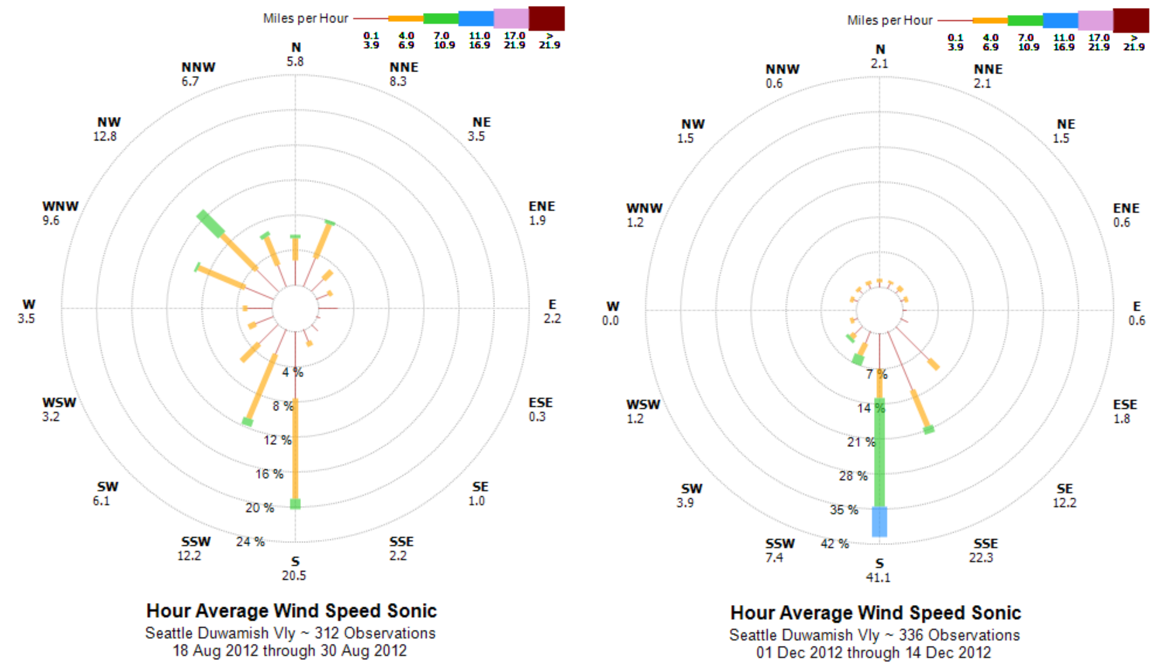

Figure 28. Wind roses from the August (left) and December (right) sampling periods. Source: Puget Sound Clean Air Agency.

Other BC Sources

Based on previous research (Schauer, 2003), BC measurements in this study were expected to reflect ambient wood smoke in addition to diesel exhaust, particularly in the winter season. However, mobile monitoring results indicated that wood smoke was not a major source of BC during the December sampling period. The presence of wood smoke is generally indicated by large differences between the ultraviolet (UV) and black carbon (BC) channel readings of the dual-channel Aethalometer®. Measurements on both channels were comparable in December. The median difference between the UV and BC channels in the core study area in December was less than 2% of the median BC value. The median ratio between winter BC and UV values was 0.98. The absence of a strong wood smoke signal in the mobile monitoring results indicates that diesel exhaust was likely the predominant source of the BC measured in the DEEDS study, even in the heating season.

CONCLUSIONS

This study demonstrated that hybrid dispersion/land-use regression models were able to identify a clear gradient in levels of diesel exhaust markers at a fine scale within individual neighborhoods. In addition, this study developed a spatial model with strong predictive ability for 1-NP, a novel marker in spatial modeling. Because 1-NP is more specific to diesel exhaust than other traffic-related pollutants previously modeled, this study was able to capture the specific sources and distribution of diesel exhaust with a higher degree of confidence. The models developed for BC and NOx, which are generally considered to be less specific markers of traffic-related air pollution, provide similar results that offer confirmation to the measured distribution of diesel pollution.

The results from the multiple pollutants measured indicate that residents of South Park and Georgetown are likely exposed to higher levels of diesel exhaust than residents of the Beacon Hill and Queen Anne comparison neighborhoods. The variation in diesel exhaust pollution levels within Seattle has significance for policy and planning. The existence of a gradient of diesel exhaust suggests that, particularly in stagnant periods, the health and environmental impacts of diesel traffic are not evenly distributed. These results reflect that residents in high intensity development areas near major roads and truck corridors likely face disproportionate impacts of diesel traffic and higher exposure to diesel exhaust. The implications of this work and this approach can also be applied to understanding neighborhood-scale community impacts of air pollution sources in Seattle and beyond.

REFERENCES

Allen R, Box M, Liu LJ, Larson TV. (2001). A cost-effective weighing chamber for particulate matter filters. *Journal of the Air and Waste Management Association*, 51(12), 1650-3.

Andreae, M. O., Gelencsér, A. (2006). Black carbon or brown carbon? The nature of light-absorbing carbonaceous aerosols. *Atmospheric Chemistry and Physics Discussions*, 6(3), 3131–3148.

Attfield, M. D., Schleiff, P. L., Lubin, J. H., Blair, A., Stewart, P. A., Vermeulen, R., Coble, J. B., Silverman, D.T.(2012). The diesel exhaust in miners study: a cohort mortality study with emphasis on lung cancer. *Journal of The National Cancer Institute*, 104(11), 869–83.

Bond, T., Anderson, T., Campbell, D. (1999). Calibration and intercomparison of filter-based measurements of visible light absorption by aerosols. *Aerosol Science & Technology*, (May 2013), 37–41.

Briggs, D., Collins, S., Elliott, P., Fischer, P., Kingham, S., Lebret, E., Pryl, K., Van Reeuwijk, H., Smallbone, K., Van Der Veen, A. (1997). Mapping urban air pollution using GIS: a regression-based approach. *International Journal of Geographical Information Science,* 11(7), 699-718.

Burton, R.M., Suh, H.H., Koutrakis, P. (1996). Spatial variation in particulate concentration within Metropolitan Philadelphia. *Environmental Science & Technology,* 30(2), 400 – 7.

Chan, P. C. (1996). NTP Technical Report on Toxicity Study of 1-Nitropyrene (CAS No. 5522-43-0) Administered by Inhalation to F344/N Rats. Research Triangle Park, NC. Retrieved from http://ntp.niehs.nih.gov/ntp/htdocs/ST_rpts/tox034.pdf.

Clougherty J. E., Wright, R.J., Baxter,L., K., Levy, J. I. (2008). Land use regression modeling of intra-urban residential variability in multiple traffic-related air pollutants. *Environmental Health,* 7(17).

Dotse, S.-Q., - Asane, J.K.,   Ofosu, F.G.(2012). Particulate Matter and Black Carbon Concentration Levels in Ashaiman, a Semi-Urban Area of Ghana.*Research Journal of Environmental and Earth Sciences,* 4(1), 20-25.

Eckel SP, Berhane K, Salam MT, Rappaport EB, Linn WS, Bastain TM, Zhang Y, Lurmann F, Avol EL, Gilliland FD. (2011). Residential traffic-related pollution exposures and exhaled nitric oxide in the children's health study. *Environmental Health Perspectives*. 119(10),1472-7.

García-Berríos, Z. I., Arce, R. (2012). Photodegradation mechanisms of 1-nitropyrene, an environmental pollutant: the effect of organic solvents, water, oxygen, phenols, and polycyclic aromatics on the destruction and product yields. *Journal of Physical Chemistry* A, 116,(14), 3652-64.

Garshick, E., Laden, F., Hart, J. E., Rosner, B., Davis, M. E., Eisen, E. A., Smith, T. J. (2008). Lung Cancer and Vehicle Exhaust in Trucking Industry Workers. *Environmental Health Perspectives*, 116, 10, 1327-1332.

Gent, J. F., Koutrakis, P., Belanger, K., Triche, E., Holford, T. R., Bracken, M. B., Leaderer, B. P. (2009). Symptoms and medication use in children with asthma and traffic-related sources of fine particle pollution. *Environmental Health Perspectives*, 117(7), 1168 – 74.

Gilroy, M., Strange, K., Yost, M. (2010). Tacoma and Seattle Area Air Toxics Evaluation. Puget Sound Clean Air Agency and University of Washington, Seattle, WA. Retrieved from http://www.pscleanair.org/news/library/reports/2010_Tacoma-Seattle_Air_Toxics_Report.pdf

Golub, G. H., Reinsch, C. (1970). Singular value decomposition and least squares solutions. *Numerische Mathematik*, 14(5), 403-420.

Gonzales, M., Qualls, C., Hudgens, E., Neas, L. (2005). Characterization of a spatial gradient of nitrogen dioxide across a United States–Mexico border city during winter. *Science of the Total Environment*, 337(1), 163-173.

Hayakawa, K., Butoh, M., Miyazaki, M. (1992). Determination of dinitro- and nitropyrenes in emission particulates from diesel and gasoline engine vehicles by liquid chromatography with chemiluminescence detection after precolumn reduction. *Analytica Chimica Acta*, 266(2), 251–256.

Hayakawa, K., Murahashi, T., Butoh, M., Miyazaki, M. (1995). Determination of 1, 3-, 1, 6-, and 1, 8-dinitropyrenes and 1-nitropyrene in urban air by high-performance liquid chromatography using chemiluminescence detection. *Environmental Science & Technology*, 29(4), 928-932.

Henderson, S.B., Beckerman, B., Jerrett, M., Brauer, M. (2007). Application of land use regression to estimate long-term concentrations of traffic-related nitrogen oxides and fine particulate matter. *Environmental Science & Technology*. 41(7); 2422-2428.

Hesterberg, T.W., Long, C.M., Bunn, W.B., Sax, S.N., Lapin, C.A., Valberg, P.A. (2009).Non-cancer
health effects of diesel exhaust: a critical assessment of recent human and animal toxicological literature. *Crit Rev Toxicol*. ,39(3), 195-227.

Hoek, G., Beelen, R., de, H. K., Vienneau, D., Gulliver, J., Fischer, P., & Briggs, D. (2008). A review of land-use regression models to assess spatial variation of outdoor air pollution. *Atmospheric Environment*, 42(33), 7561-7578.

International Agency for Research on Cancer. (1985). 1-Nitropyrene (pp. 321–358). International Agency for Research on Cancer Monograph. Retrieved from: http://monographs.iarc.fr/ENG/Monographs/vol46/mono46-19.pdf

International Agency for Research on Cancer. (2012). IARC: DIESEL ENGINE EXHAUST CARCINOGENIC. Press Release. Retrieved from http://www.iarc.fr/en/media-centre/pr/2012/pdfs/pr213_E.pdf

Jerrett, M., Arain, A., Kanaroglou, P., Beckerman, B., Potoglou, D., Sahsuvaroglu, T., Morrison, J., Giovis, C. (2005). A review and evaluation of intraurban air pollution exposure models. *Journal of Exposure Analysis and Environmental Epidemiology*, 15(2), 185–204.

King County (2010). South Park Bridge TIGER II Grant - Traffic analysis summary. Retrieved 5/28/2013, 2010, from http://kingcounty.gov/transportation/ TIGERII/EconomicsAndJobs/TrafficAnalysis.aspx

King County (2012). KCGIS data download. Retrieved 02/01/2013, 2012, from http://www5.kingcounty.gov/gisdataportal/Default.aspx

Kinney PL, Aggarwal M, Northridge ME, Janssen NA, Shepard P. (2000). Airborne concentrations of PM(2.5) and diesel exhaust particles on Harlem sidewalks: a community-based pilot study. *Environmental Health Perspectives* 108(3), 213-8.

Larson, T., Henderson, S. B., Brauer, M. (2009). Mobile monitoring of particle light absorption coefficient in an urban area as a basis for land use regression. *Environmental Science & Technology*, 43(13), 4672-8.

Levaggi DA, Siu W, Feldstein M, Kothny EL. (1972). Quantitative separation of nitric oxide from nitrogen dioxide at atmospheric concentration ranges. *Environmental Science & Technolology*, 6, 250-252.

Lindstrom J., Szpiro A.A., Sampson P.D., Sheppard L., Oron A., Richards M., Larson T. A Flexible Spatio-Temporal Model For Air Pollution: Allowing For Spatio-Temporal Covariates. *Environmental and Ecological Statistics* (in press).

Magee Scientific. (2010). Introducing the new microAeth ® Model AE52 (pp. 1–2). Berkeley, CA.

Mavko, M. E., Tang, B., George, L. A. (2008). A sub-neighborhood scale land use regression model for predicting NO_2. *Science of the Total Environment*, 398(1), 68-75.

McConnell, R., Islam, T., Shankardass, K., Jerrett, M., Lurmann, F., Gilliland, F., Gauderman, J. (2010). Childhood incident asthma and traffic-related air pollution at home and school. *Environmental Health Perspectives*, 118(7), 1021 - 6.

Mercer, L. D., Szpiro, A. A., Sheppard, L., Lindström, J., Adar, S. D., Allen, R. W., Avol, E. L., Oron, A.P., Larson, T., Liu, L.J., Kaufman, J.D. (2011). Comparing universal kriging and land-use regression for predicting concentrations of gaseous oxides of nitrogen (NOx) for the Multi-Ethnic Study of Atherosclerosis and Air Pollution (MESA Air). *Atmospheric Environment* ,45(26), 4412–4420.

Miller-Schulze J.P.,, Paulsen M., Toriba A., Tang, N., Hayakawa, K., Tamura, K., Dong, L., Zhang, X., Simpson, C.D.. (2010) Exposures to particulate air pollution and nitro-polycyclic aromatic hydrocarbons among taxi drivers in Shenyang, China. *Environmental Science & Technology*,44(1), 216-221.

United States Geological Survey. (2006). Multi-Resolution Land Characteristics Consortium. National Land Cover Database 2006 (NLCD2006) Product Legend. U.S. Geological Survey. Retrieved 5/9/2013 from http://www.mrlc.gov/nlcd06_leg.php.

Murakami, M., Yamada, J., Kumata, H., Takada, H. (2008). Sorptive behavior of nitro-PAHs in street runoff and their potential as indicators of diesel vehicle exhaust particles. *Environmental Science & Technology*, 42(4), 1144–50.

Nightingale, J.A., Maggs, R., Cullinan, P., Donnelly, L.E., Rogers, D.F., Kinnersley, R., Chung, K.F., Barnes, P.J., Ashmore, M., Newman-Taylor, A. (2000). Airway inflammation after controlled exposure to diesel exhaust particulates. Am J Respir Crit Care Med, 162(1),161-6.

Nordenhäll, C., Pourazar, J., Blomberg, A., Levin, J.O., Sandström, T., Adelroth, E. (2000). Airway inflammation following exposure to diesel exhaust: a study of time kinetics using induced sputum. *European Respiratory Journal*,15(6), 1046-51.

Novotny, E., Bechle, M. (2011). National satellite-based land-use regression: NO2 in the United States. *Environmental Science & Technology*, (2), 4407–4414.

Ogawa & Co. (2006). NO, NO2, NOx and SO2 Sampling Protocol Using the Ogawa Sampler, Ogawa & Co., USA, Inc.

Olsson, A. C., Gustavsson, P., Kromhout, H., Peters, S., Vermeulen, R., Brüske, I., Pesch, B., et al. (2011). Exposure to Diesel Motor Exhaust and Lung Cancer Risk in a Pooled Analysis from Case-Control Studies in Europe and Canada. *American Journal of Respiratory and Critical Care Medicine*, 183(7), 941–948.

Palcisko, G. (2008). Health Consultation: Summary of Results of Duwamish Valley Regional Modeling and Health Risk Assessment. U.S. Department of Health and Human Services, Atlanta, GA.

Puget Sound Regional Council. (2008). PSRC Travel Model Documentation (for Version 1.0). Puget Sound Regional Council, Seattle, WA.

Puget Sound Sage. (2009). Community Health Impact Survey Results: Port of Seattle Operations Hazardous to Health in Georgetown and South Park. Seattle, WA. Retrieved from http://pugetsoundsage.org/downloads/Community Health Impact Survey Overview.pdf.

Rao, V., Somers, J. H. (2010). Black Carbon as a Short-Lived Climate Forcer : A Profile of Emission Sources and Co-Emitted Pollutants. U.S. Environmental Protection Agency.

Ross, Z., Jerrett, M., Ito, K., Tempalski, B., Thurston, G.D. (2007). A land use regression for predicting fine particulate matter concentrations in the New York City region. *Atmospheric Environment*, 41(11), 2255-69.

Ryan, P. H., LeMasters, G. K., Levin, L., Burkle, J., Biswas, P., Hu, S., Grinshpun, S.,Reponen, T. (2008). A land-use regression model for estimating microenvironmental diesel exposure given multiple addresses from birth through childhood. *Science of the Total Environment*, 404(1), 139-147.

Sampson P.D., Richards, M., Szpiro, A. A., Bergen, S., Sheppard, L., Larson, T.V., Kaufman, J.D. (2013). A Regionalized National Universal Kriging Model using Partial Least Squares Regression for Estimating Annual PM2.5 Concentrations in Epidemiology. *Atmospheric Environment,* 75, 383-392.

Sampson, P. D., Szpiro, A. A., Sheppard, L., Lindström, J., Kaufman, J. D. (2011). Pragmatic estimation of a spatio-temporal air quality model with irregular monitoring data. *Atmospheric Environment*, 45(36), 6593-6606.

Schauer JJ. (2003). Evaluation of elemental carbon as a marker for diesel particulate matter. *Journal of Exposure Analysis and Environmental Epidemiology*. ,6,443-53.

Silverman, D. T., Samanic, C. M., Lubin, J. H., Blair, A. E., Stewart, P. A., Vermeulen, R., Coble, J. B., Rothman, N., Schleiff, P.L., Travis, W.D., Ziegler, R.G., Wacholder, S., Attfield, M.D. (2012). The Diesel Exhaust in Miners study: a nested case-control study of lung cancer and diesel exhaust. *Journal of the National Cancer Institute*,104, 855–68

Sydbom, A., Blomberg, A., Parnia, S., Stenfors, N., Sandström, T., Dahlén, S. E. (2001). Health effects of diesel exhaust emissions. The European respiratory journal : official journal of the European Society for Clinical Respiratory Physiology, 17(4), 733–46.

Tibshirani, R. (1996). Regression Shrinkage and Selection via the Lasso. *Journal of the Royal Statistical Society. Series B* (methodological), 58, 1, 267-288.

U.S. Census Bureau. (2010). U.S. Census Bureau, Census 2010 Summary File 1. Retrieved 6/26/2012, from http://factfinder2.census.gov

U.S. Census Bureau (2010). U.S. Census Bureau, 2006-2010 American Community Survey. Retrieved 6/26/2012, from http://factfinder2.census.gov

U.S. EPA. (1995). User's Guide to CAL3QHC Version 2.0: A Modeling Methodology for Predicting Pollutant Concentration Near Roadway Intersections . U.S. Environmental Protection Agency, Research Triangle Park, NC.

U.S. EPA (1998). Quality assurance guidance document 2.12 monitoring PM2.5 in ambient air using designated reference or class I equivalent methods. In U.S. Environmental Protection Agency, N.E.R.L., Ed. 1998. http://www.epa.gov/ttn/amtic/files/ambient/pm25/qa/m212covd.pdf

U.S. EPA. (2012). Report to Congress on Black Carbon (pp. 115–137). U.S. Environmental Protection Agency, Research Triangle Park, NC.

U.S. EPA. (2012). The National Ambient Air Quality Standards: Overview of EPA's Revisions to the Air Quality Standards for Particle Pollution (Particulate Matter.) http://www.epa.gov/airquality/particlepollution/2012/decfsoverview.pdf

Van den Braken-van Leersum, A. M., Tintel, C., van't Zelfde, M., Cornelisse, J.; Lugtenburg, J. (1987) *Recl. Trav. Chim. Pays−Bas*, 106, 120−128.

Wilton, D., Szpiro, A., Gould, T., Larson, T. (2010). Improving spatial concentration estimates for nitrogen oxides using a hybrid meteorological dispersion/land use regression model in Los Angeles, CA and Seattle, WA. *Science of the Total Environment*, 408(5), 1120–1130.

Yang, M., Howell, S. G., Zhuang, J., Huebert, B. J. (2008). Attribution of aerosol light absorption to black carbon, brown carbon, and dust in China -Interpretations of atmospheric measurements during EAST-AIRE. Atmospheric Chemistry and Physics Discussions, 8, 3, 10913-10954.